Biomedicine & Pharmacotherapy 149 (2022) 112910

Contents lists available at ScienceDirect

Biomedicine & Pharmacotherapy

journal homepage: www.elsevier.com/locate/biopha

BMP7-based peptide agonists of BMPR1A protect the left ventricle against pathological remodeling induced by pressure overload

Ana B. Salido-Medina [a], Aritz Gil [a,b], Víctor Expósito [a,b], Fernando Martínez [c,d], Juan M. Redondo [d,e], María A. Hurlé [a,f], J.Francisco Nistal [a,d,g,h,*], Raquel García [a,f,**]

[a] Instituto de Investigación Sanitaria Valdecillla (IDIVAL), Santander, Spain
[b] Servicio de Cardiología, Hospital Universitario Marqués de Valdecilla (HUMV), Santander, Spain
[c] Bioinformatics Unit, Centro Nacional de Investigaciones Cardiovasculares (CNIC), Madrid, Spain
[d] Centro de Investigación Biomédica en RED en Enfermedades Cardiovasculares (CIBERCV), Madrid, Spain
[e] Gene regulation in cardiovascular remodeling and inflammation group, Centro Nacional de Investigaciones Cardiovasculares (CNIC), Madrid, Spain
[f] Departamento de Fisiología y Farmacología, Facultad de Medicina, Universidad de Cantabria, Santander, Spain
[g] Departamento de Ciencias Médicas y Quirúrgicas, Facultad de Medicina, Universidad de Cantabria, Santander, Spain
[h] Servicio de Cirugía Cardiovascular, Hospital Universitario Marqués de Valdecilla (HUMV), Santander, Spain

ARTICLE INFO

Keywords:
Aortic stenosis
Pressure overload
Myocardial remodeling
BMP7
BMPR1A

ABSTRACT

Aortic stenosis (AS) exposes the left ventricle (LV) to pressure overload leading to detrimental LV remodeling and heart failure. In animal models of cardiac injury or hemodynamic stress, bone morphogenetic protein-7 (BMP7) protects LV against remodeling by counteracting TGF-β effects. BMP receptor 1A (BMPR1A) might mediate BMP7 antifibrotic effects. Herein we evaluated BMP7-based peptides, THR123 and THR184, agonists of BMPR1A, as cardioprotective drugs in a pressure overload model. We studied patients with AS, mice subjected to four-week transverse aortic constriction (TAC) and TAC release (de-TAC). The LV of AS patients and TAC mice featured *Bmpr1a* downregulation. Also, pSMAD1/5/(8)9 was reduced in TAC mice. Pre-emptive treatment of mice with THR123 and THR184, during the four-week TAC period, normalized pSMAD1/5/(8)9 levels in the LV, attenuated overexpression of remodeling-related genes (*Col 1α1*, *β-MHC*, *BNP*), palliated structural damage (hypertrophy and fibrosis) and alleviated LV dysfunction (systolic and diastolic). THR184 administration, starting fifteen days after TAC, halted the ongoing remodeling and partially reversed LV dysfunction. The reverse remodeling after pressure overload release was facilitated by THR184. Both peptides diminished the TGF-β1-induced hypertrophic gene program in cardiomyocytes, collagen transcriptional activation in fibroblasts, and differentiation of cardiac fibroblasts to myofibroblasts. Molecular docking suggests that both peptides bind with similar binding energies to the BMP7 binding domain at the BMPR1A. The present study results provide a preclinical proof-of-concept of potential therapeutic benefits of BMP7-based small peptides, which function as agonists of BMPR1A, against the pathological LV remodeling in the context of aortic stenosis.

1. Introduction

Degenerative aortic valve stenosis (AS) is an ageing-related disorder that is the most prevalent adult heart valve disease requiring surgery in developed countries [1]. AS subjects the left ventricle (LV) to a slowly progressing pressure overload that elicits a myocardial remodeling response. The process of cardiac remodeling is usually progressive and involves molecular, cellular, microvascular and interstitial phenomena that manifest as phenotypic changes in size, shape, structure, and function [2,3]. LV hypertrophy, over time, becomes pathological; detrimental microstructural features, including interstitial and perivascular fibrosis, capillary rarefaction, and cardiomyocyte apoptosis, resulting in deterioration of LV diastolic and systolic functions up to the stage of overt heart failure [2,3].

Aortic valve replacement (via open surgery or transcatheter) is currently the only effective therapy for symptomatic patients with AS

* Correspondence to: Dpto. Ciencias Médicas y Quirúrgicas, Facultad de Medicina, Universidad de Cantabria, Hospital Universitario Marqués de Valdecilla (HUMV), E-39011 Santander, Spain.
** Correspondence to: Dpto. Fisiología y Farmacología, Facultad de Medicina, Universidad de Cantabria, E-39011 Santander, Spain.
E-mail addresses: jfnistal@gmail.com (J.Francisco Nistal), garcialr@unican.es (R. García).

https://doi.org/10.1016/j.biopha.2022.112910
Received 17 January 2022; Received in revised form 28 March 2022; Accepted 29 March 2022
Available online 4 April 2022

[4], no effective medical treatments are available to delay or avoid surgery. The functional and structural changes in the LV can be alleviated by valve replacement (reverse remodeling). Still, the degree and completeness of postoperative recovery of the heart and, therefore, the long-term functional outcome of the patients depends on the severity of the structural alterations developed during the evolution of AS before surgery [5,6].

The transforming growth factor β (TGF-β) superfamily encompasses a large group of pleiotropic cytokines, including TGF-βs, activins, and bone morphogenetic proteins (BMPs), which are critically involved in embryogenesis and development and the maintenance of adult tissue homeostasis. Alterations in TGF-β superfamily pathways often result in severe human diseases [7,8].

The aberrant interplay between TGF-βs and BMPs plays a central pathophysiological role in chronic fibrotic diseases of most organs, which ultimately leads to loss of function of the affected organ.[9,10] In particular, TGF-β1 acts as a powerful promoter of fibrosis by inducing endothelial-to-mesenchymal transition, fibroblast proliferation, and transdifferentiation of these cells into myofibroblasts [10–15]. Conversely, BMP7 (also termed osteogenic protein-1, OP-1) counteracts TGF-β1-induced profibrogenic effects. Thus, rhBMP7 has proven efficacious in various experimental models of clinically relevant progressive fibrotic processes of organs such as the kidneys, liver, lungs, joints and heart [16–22].

In the context of the heart under pressure overload stress, our group and others have shown in mice subjected to transverse aortic constriction (TAC) that rhBMP7 attenuates the structural damage of the LV (fibrosis and hypertrophy), halts remodeling progression, and facilitates reverse remodeling after releasing the hemodynamic overload [11,19]. Conversely, blunting BMP7 signaling through pharmacological or genetic strategies potentiates TAC-induced myocardial hypertrophy and fibrosis [19].

BMP canonical signaling in target cells involves type I and type II receptor tetrameric complexes. Unlike TGF-β ligands, BMPs preferentially bind type I receptors and recruit type II receptors. The constitutively active type II receptor transphosphorylates and activates the type I receptor upon forming the heterotetrameric complex. Activated BMP type I receptors (BMPRI), often referred to as activin-like kinases (ALKs), have serine/threonine kinase activity, and their canonical cell effectors are the phosphorylated SMAD1/5/(8)9 transcription factors [8,23]. In particular, BMP7 binds BMPR1A (ALK3), BMPR1B (ALK6), and the activin A receptor type 1 ACVR1 (ALK2). Notably, several reports demonstrate the involvement of BMPR1A mediated signaling in the protective role of BMP7 against renal fibrosis [17,24].

The clinical use of rhBMP7 tissue-engineered products has been approved by US and EU agencies to induce localized osteogenesis in orthopedic and maxillofacial applications [7]. However, the potential therapeutic benefit of restoring BMP7 function using systemic rhBMP7 is hampered by bioavailability concerns, induction of neutralizing autoantibodies against BMPs, and a range of potential adverse effects [7,25]. However, based on promising preclinical results, Sugimoto et al. have generated a library of BMP7-derived small peptides, agonists of BMPR1A, whose lead candidate THR123 exhibits robust antifibrotic and regenerative effects in several experimental models of acute and chronic kidney diseases [17]. In addition, THR-184, another synthetic peptide from the family of modulators of the BMP7 pathway, was evaluated in clinical studies of renal injury (NIH, ClinicalTrials.gov Identifier: NCT01830920) [26].

In the present study, we investigated whether targeting BMPR1A signaling with THR123 and THR184 in the heart under hemodynamic stress might be a potential pharmacological strategy to prevent, halt, or reverse pathological myocardial remodeling.

2. Materials and methods

2.1. Pressure overload studies in mice

The experiments were performed in 16–20 week old male and female C57BL/6 mice. The study was approved by the University of Cantabria Institutional Laboratory Animal Care and Use Committee and was conducted according to directive 2010/63/E.U. guidelines of the European Parliament. The number of animals per group was the minimum necessary to achieve statistically significant differences. All animals received humane care, and all effort was made to minimize animal suffering.

2.1.1. Transverse aortic constriction (TAC) surgery and release (de-TAC)

We randomized male and female C57BL/6 mice to receive either TAC or sham operation. TAC surgery was performed using the customized technique described by Merino et al. which provides functionally equivalent levels of pressure overload regardless of the somatometry of the animals, allowing for a fair comparison between male and female mice.[27].

After TAC surgery, the animals were followed up for four weeks. In a series of mice, the constriction was released (de-TAC mice)[28] and these mice were followed up for one week. In termination studies, the mice were euthanised by decapitation under ketamine-xylazine anesthesia. The heart was harvested, and the LV was dissected and weighed before snap-freezing in liquid nitrogen or fixing in 4% paraformaldehyde. The lungs were retrieved and weighed immediately, and after drying in an oven 65 ºC/72 h.

2.1.2. Treatments

THR123 and THR184 peptides (CanPeptide, Quebec, Canada) were administered intraperitoneally (5 μg/g/day) during (i) the entire 4-week TAC period (Fig. 1A) and (ii) the 3rd and 4th weeks after TAC (Fig. 1B) when LV remodeling was already ongoing. THR184 was administered (10 μg/g/day) during one week after de-TAC, to evaluate LV reverse remodeling after the release of pressure overload (Fig. 1C).

2.1.3. Echocardiography

Mice underwent echocardiographic analysis at baseline and weekly after TAC or sham surgery. Transthoracic echocardiography was performed under sedation with isoflurane (2.5%), with high-resolution ultrasound equipment [Vevo-770 (Fujifilm-VisualSonics, Toronto, ON, Canada) with a 40 MHz center frequency transducer. The operator was blinded to the type of drug or inactive treatment received by the animals. Transcoarctational pressure gradients were measured with pulsed-wave Doppler analysis at the distal arch and confirmed with continuous-wave Doppler interrogation (Philips-HP Sonos 5500 console with a 12 MHz transducer). LV end-diastolic and end-systolic internal diameters, interventricular septum, and LV posterior wall thicknesses were measured in 2D guided M-mode recordings in the short axis left parasternal window, according to the recommendations of the American Society of Echocardiography. Cardiac mass was estimated with Devereux's formula. Mitral annular plane systolic excursion (MAPSE) was used to estimate the LV systolic function in the long axis. The ratio of the peak early transmitral flow velocity (E) to peak early myocardial tissue velocity (e') was measured with tissue Doppler imaging. E/e' estimates the LV filling pressures, and it was used to assess diastolic function.

2.2. Pressure overload studies in patients

The study followed the Declaration of Helsinki guidelines for biomedical research involving human participants and was approved by our institutional ethics and clinical research committee. All patients were informed verbally and through printed material about the nature of the study and provided written informed consent.

The study was performed in a cohort of 33 patients diagnosed with

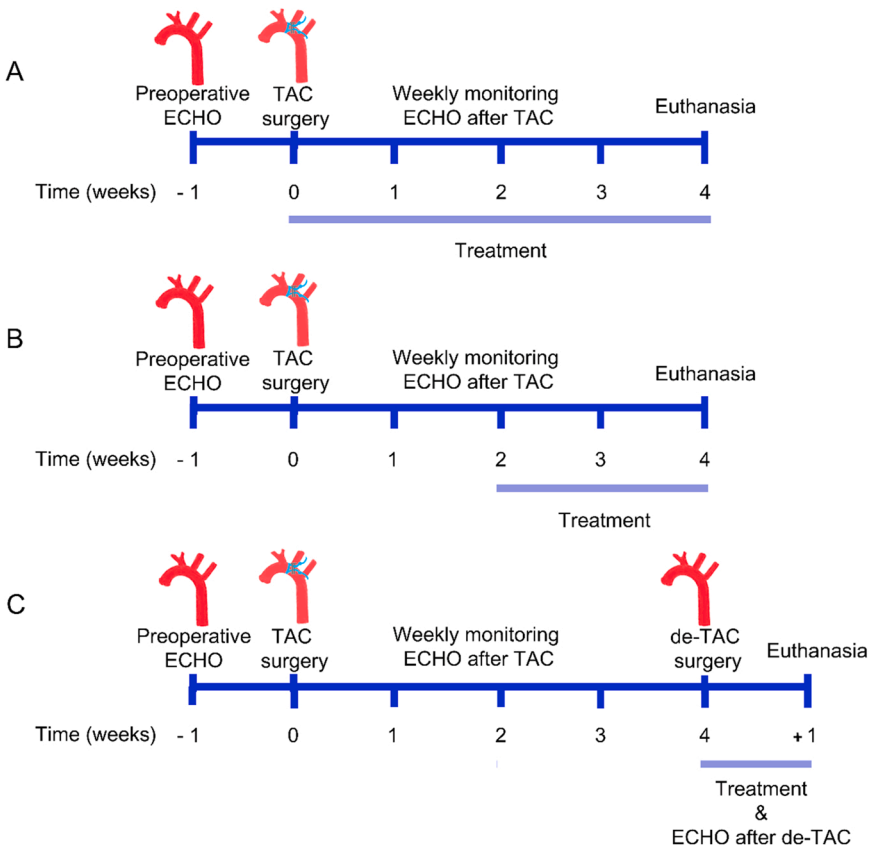

Fig. 1. Diagram of experimental groups with the schedule of surgeries, treatments, and echocardiographic studies. (A) THR123, THR184 or saline treatment begins immediately after the TAC surgery and extends throughout the follow-up period. (B) Treatment from the 3rd week post-TAC. THR123 and THR184 peptides were administered intraperitoneally (5 μg/g/day). (C) Treatment with THR184 (10 μg/g/day) or saline during one week after de-TAC surgery, starting at the moment of de-TAC. TAC, transverse aortic constriction.

isolated severe AS and undergoing aortic valve replacement surgery at the University Hospital Marqués de Valdecilla in Santander, Spain. Patients with aortic or mitral regurgitation greater than mild, significant coronary stenosis > 50%, previous cardiac operations, malignancies, or poor renal or hepatic function were deemed ineligible for the study. The control group comprised a cohort of ten surgical patients with pathologies not associated with LV pressure or volume overload, coronary heart disease, or cardiomyopathies. The clinical and demographic characteristics of the AS and control groups are shown in Table S1.

During the surgical procedure, intraoperative subepicardial biopsies (40 mg × 3) were obtained from the LV lateral wall with a Tru-Cut™ needle. A single surgeon collected all samples, in a protocolised manner, from the same location in the obtuse margin of the heart.

2.3. Studies in cultured cells

2.3.1. NIH-3T3 fibroblasts and H9C2 cardiomyocytes

NIH-3T3 fibroblast and H9C2 cardiomyocyte cell lines (ATCC) were cultured in DMEM supplemented with 10% DBS and 10% FBS, respectively, and 100 U/ml penicillin-streptomycin, at 37 °C under 5% CO_2. The cells were seeded in 12-well plates (10^5 cells/well) and cultured for 24 h in DMEM supplemented with 0.5% serum. In a series of experiments, the BMP type I receptor inhibitors DMH2 [(10 nM); Ki values < 1, 5.4 and 43 nM for BMPR1B, BMPR1A, and ACVR1, respectively (Tocris, Bristol, UK)] or the dorsomorphin derivate small molecule LDN-193189 [(30 nM); IC50 = 5 nM and 30 nM, for ACVR1 and BMPR1A, respectively (Abcam, Cambridge, UK)] were used to block BMP type I receptors. After 4 h, the cells were incubated with TGF-β1 (10 ng/ml; R&D Systems) for 24 h. Then THR123 (1 μg/ml) or THR184 (1 μg/ml) was added. Dose-response experiments were performed to determine the optimum concentrations of the peptides, and a dose of 1 μg/ml of each peptide was subsequently used in all experiments. The cells were collected the following day, processed for mRNA isolation, and analysed by qPCR as described below.

H9C2 cardiomyocytes seeded on glass coverslips were incubated for 24 h with DMEM supplemented with 0.5% serum containing TGF-β1 (10 ng/ml), TGF-β1 (10 ng/ml) plus THR123 (1 μg/ml) or TGF-β1 (10 ng/ml) plus THR184 (1 μg/ml). After fixation in paraformaldehyde (4% in PBS), cellular actin was stained with FITC-conjugated phalloidin (1% in PBS) for 30 min. Slides were mounted in Vectashield with DAPI (Vector Labs). A Zeiss Axioplan II microscope was used to acquire the images, and cardiomyocyte diameter was measured using ImageJ software. Results are reported as the diameter of 45 cells per treatment, measured in two different experiments.

2.3.2. MTS colorimetric proliferation assay

For MTS proliferation assays, 10^4 NIH-3T3 and H9C2 cells per well were seeded in a 96-well cell culture plate for 48 h. THR123 or THR184 was assessed between 0 and 10 μg/ml. After 24 h, the tetrazolium salt MTS was added to the wells, and the plate was incubated at 37 °C for 3 h in the dark. The absorbance was read at 490 nm with a Spark Multimode Microplate Reader (Tecan Trading AG).

2.3.3. Cardiac primary fibroblasts

Mice were decapitated under anesthesia with isoflurane (4%) at 4–6 weeks postnatally, and the hearts were excised. The tissue was subjected to enzymatic digestion as previously described.[14] Fibroblasts were grown to 70% confluence before growth arrest was induced with serum-free medium for 24 h. The cells were then incubated with TGF-β1 (10 ng/ml; R&D Systems), TGF-β1 (10 ng/ml) plus THR123 (1 μg/ml) or TGF-β1 (10 ng/ml) plus THR184 (1 μg/ml) for 48 h. We used the minimum dose of TGF-β1 required to promote myofibroblast differentiation. [29].

2.3.4. Proliferation assay

Cell proliferation was measured by BrdU incorporation using

Proliferation Assay Kit (Merck BrdU Cell Proliferation Assay Kit) according to the manufacturer's instructions. Briefly, mice cardiac primary fibroblasts were seeded (5×10^4) in 96 well plates for 24 h and then incubated in DMEM medium supplemented with 0,5% of serum for 24 h. Then cells were incubated with TGF-β1 (10 ng/ml), TGF-β1 (10 ng/ml) plus THR123 (1 μg/ml) or TGF-β1 (10 ng/ml) plus THR184 (1 μg/ml) for 24 h. BrdU diluted medium was added to each well in 96 well plates after 6 h TGF-β1 stimulation.

2.4. Wound healing assay

Mice cardiac primary fibroblasts were incubated in complete media at 37 ºC in 5% CO_2 until a regular monolayer was formed. After incubation in medium supplemented with 0,5% of serum for 24 h, straight scratches for each well were made with a 200 μl pipette tip. The wells were then incubated with the different treatments described above. Pictures were captured at 0 h and 10 h time points, and then the migration area was analysed by Image J.

2.5. mRNA expression

Total RNA was obtained with TRIzol (Invitrogen, CA, USA). Real-time qPCR was conducted with specific TaqMan assays (Thermo Fisher, MA, USA) for the following transcripts: *Bmpr1a*, *Acvr1*, *Bmpr1b*, *Collagen 1a1* (*Col 1a1*), *β-myosin heavy chain* (*β-MHC*), *B-type natriuretic peptide* (*BNP*) and *α2-Actin* (*Acta-2*). mRNA expression levels were normalized to ribosomal *18S* RNA. Triplicate transcript levels were determined in a minimum of three independent experiments.

2.6. Histology

Hearts were fixed in paraformaldehyde 4% for 24 h and embedded in paraffin. Four short-axis sections (4 μm) at the level of the papillary muscles, from a minimum of three mice per experimental condition, were stained with Masson's trichrome. Digital photographs of the complete LV sections were captured with a camera (Axiocam MRc5, Zeiss, Oberkochen, Germany) attached to a Zeiss Axioplan microscope. The fractional area of fibrosis was determined using ImageJ software (National Institute of Health, MD, USA). The results are expressed as the percentage of the blue-stained regions divided by the total LV myocardial area. The minor diameter of cardiomyocytes was measured (three fields per mouse in a minimum of three mice per group).

2.7. Immunostaining

Primary mouse cardiac fibroblasts were fixed in 4% paraformaldehyde for 15 min. After permeabilisation with 0.3% PBS-Triton X-100 (Sigma-Aldrich,) for 15 min at room temperature and blocking with 1% BSA (Sigma-Aldrich), the cells were incubated with chicken anti-vimentin (Abcam, ab24525) and mouse anti-α-SMA (Abcam, ab7817) overnight at 4 °C. After being washed with PBS, the cells were incubated for 30 min at room temperature with the specific secondary antibodies conjugated with FITC or Cy3 (Jackson ImmunoResearch, Cambridge, UK). Confocal images were obtained with an LSM510 laser scanning microscope (Zeiss, Germany) with a 20 × objective. Images were post-processed in Adobe Photoshop CS6 software (Adobe Systems, Mountain View).

2.8. Western blotting

Whole-cell lysates were prepared from mouse LV samples and primary fibroblasts. Equal amounts of protein (LV: 30 μg; fibroblasts: 4 μg) were resolved on 10% (LV) or 12.5% (fibroblasts) sodium dodecyl sulfate-polyacrylamide (SDS-PAGE) gel and transferred onto polyvinylidene difluoride (PVDF) membranes (Bio-Rad Lab., California, USA) using a Mini Trans-Blot Electrophoresis Transfer Cell (Bio-Rad Lab., California, USA). The primary antibodies used were mouse monoclonal antibody to α-SMA (Abcam, ab7817), rabbit polyclonal antibody to pSMAD1/5/(8)9 (Santa Cruz Biotechnology, sc-12353), mouse monoclonal antibody to α-tubulin (Sigma-Aldrich, T5168), and mouse monoclonal antibody to GAPDH (Santa Cruz Biotechnology, sc-32233) After incubation with the appropriate peroxidase-conjugated secondary antibodies, immunoreactivity was detected using the ECL Advance kit (GE Healthcare). Blot quantification was performed by densitometry using ImageJ software (National Institute of Health, MD, USA). The results were expressed as the optical density of the sample dots normalized to that obtained for α-tubulin or GAPDH. Samples from 3 subjects per group were tested in three independent experiments.

2.9. Statistics

Data are expressed as means ± SEM. Differences between two independent groups were assessed with Student's t-test. Differences between multiple groups were analysed with one-way or two-way ANOVA followed by the Bonferroni post hoc test. Correlations were performed using Pearson's correlation analysis. The significance level was $p < 0.05$. GraphPad Prism 5 (GraphPad Inc, CA, USA) software was used for statistical analysis.

2.10. Molecular docking

3D structure-based *in silico* strategies were used to assess the interactions of BMP7 and the small molecules THR123, THR184 onto the human BMPR1A. The 3D structure of the complex formed by BMPR1A bound to BMP7 is lacking in Protein Data Bank (Worldwide Protein Data Bank (wwPDB.org)). Therefore, we generated a template of the human BMPR1A receptor in its bonded form with BMPs based on the complex BMP2-BMPR1A described by Keller et al. [30] We performed a structural alignment between BMP2 (PDB ID: 2QJB) and BMP7 (PDB ID: 1LXI) in the presence of BMPR1A (PDB ID: 2QJB), and the root-mean-square deviation (RMSD) was lower than 1 Å, which meant that, structurally, both cytokines were practically identical. Based on this structural similitude, we eliminated the BMP2 molecule and generated a template of BMP7 with BMPR1A.

PEPstrMOD (osddlinux.osdd.net/Raghava/pepstrmod) was used for generating the 3D structure of the peptides based on the amino acid sequence (Table S2).

Ligand-protein and protein-protein docking were conducted using the free web servers ClusPro (cluspro.bu.edu) and Rosetta Flex-pep-Dock (flexpepdock.furmanlab.cs.huji.ac.il). ClusPro applies rigid-body docking and searches the possible complexes according to shape complementarity, whereas Flex-pep-dock allows for flexibility in the peptides, both backbone and sidechains, and receptor sidechains during docking. InterfaceAnalyzer from RosettaCommons (rosettacommons.org) was chosen to identify the residues in the binding interfaces between proteins. PyMOL (PyMOL Molecular Graphics System, Version 2.3.4 Schrödinger, LLC) was used for the final representation of molecular complexes.

3. Results

3.1. Studies in vivo and ex vivo

3.1.1. Expression of BMP7 type I receptors in the LV myocardium from mice and humans and their regulation under pressure overload

BMPR1A receptors have been associated with the protective effects of BMP7 in experimental models of pathological fibrosis [17,19,24]. However, the myocardial expression and regulation under hemodynamic stress of the type I receptors involved in BMP7 signaling have not been explored. Herein, we determined the mRNA levels of *Bmpr1a*, *Bmpr1b* and *Acvr1* in the LV in mice and humans by qPCR. *Bmpr1a* was the most expressed type 1 receptor in the healthy murine myocardium

and was significantly downregulated in the LV subjected to 4 weeks of TAC compared with sham mice (Fig. 2A). In a previous study, we demonstrated in TAC mice that the expression of *Bmpr1a* in the LV correlates inversely with remodeling-related gene expression and hypertrophy developed, while the relationship is direct with LV functional systolic parameters [19]. Consistently with these findings, downregulation of *Bmpr1a* was also observed in the LV of patients with AS compared with surgical controls (Fig. 2B). Furthermore, the inverse correlation of *Bmpr1a* transcript levels with both preoperative interventricular septum thickness ($n = 33$; $r = -0.39$; $p = 0.025$) and expression of the hypertrophy marker *β-MHC* ($n = 33$; $r = -0.4$; $p = 0.022$) (Fig. S1) supports a role of altered BMPR1A signaling also in maladaptive myocardial remodeling in AS patients.

3.1.2. *Effects of the treatment with THR123 and THR184 on the myocardial remodeling response induced by pressure overload in mice*

We investigated whether pharmacological modulation of BMPR1A signaling with the BMP7 analogs THR123 and THR184 effectively prevents, halts, or reverses the pathological LV remodeling under hemodynamic stress.

3.1.2.1. Preventive treatment with THR123 and THR184 starting on the day of TAC surgery. Male and female mice undergoing TAC or sham surgery received daily injections of saline, THR123, or THR184 (5 μg/g, i.p.) from the day of surgery until a 4-week follow-up period; echocardiographic studies were performed weekly. After completing the follow-up, mice were euthanized. The LVs were harvested, weighed, and processed for qPCR, histology, or western blotting.

After TAC surgery, the average transcoarctation pressure gradients reached similar values (~60 mmHg) in all experimental groups (Fig. S2). Both THR123 and THR184, compared with saline, significantly attenuated the LV morpho-functional remodeling induced by 4-week TAC in male and female mice, as determined echocardiographically weekly (Fig. 3) and gravimetrically at 4 weeks endpoint (Fig. S3). As shown in Fig. 3, the time course of echocardiographic changes in indexed LV mass (LVMI) (Fig. 3A & B) and in the interventricular septum thickness (ΔIVS) (Fig. 3C & D) indicated a lower degree of LV hypertrophy in the TAC mice treated with either drug, compared to saline. Moreover, treated mice exhibited lower LV systolic and diastolic deterioration, as shown by the MAPSE (Fig. 3E & F) and E/e', respectively (Fig. 3G & H). In sham mice, neither THR123 nor THR184 caused significant changes in any echocardiographic morpho-functional parameter (Table S3).

The degree of cardiac dysfunction was also evaluated through the wet lung weight, indicative of lung edema. As shown in Fig. S4, no significant increase in lung water content was observed in any experimental group compared to sham mice, indicating the absence of congestive lung signs at 4 weeks TAC [31].

The treatment with THR123 or THR184 reduced the myocardial overexpression of remodeling-associated genes induced by 4 weeks of pressure overload, including the fibrosis marker *Col 1a1*, the hypertrophy marker *β-MHC* and the heart failure marker *BNP* [32] four weeks after TAC (Fig. 4A, B & C). In addition, LV sections stained with Masson's trichrome (Fig. 4D, E & F) showed a significantly lower fibrotic area of the LV and a smaller average diameter of cardiomyocytes in TAC mice treated with THR123 or THR184, compared with saline. Detailed cross-sectional area of cardiomyocytes in mice LV sections are shown in Fig. S5A.

Overall, our data indicated that sustained treatment with THR123 and THR184 during four weeks of pressure overload attenuated the structural (hypertrophy and fibrosis) and functional (systolic and diastolic) remodeling of the LV in mice of both sexes.

3.1.2.2. Treatment with THR123 or THR184 during the 3rd and 4th weeks after TAC. We next assessed whether BMPR1A agonists might protect against the progression of the ongoing structural remodeling of the LV and its functional consequences. To this end, TAC mice received daily injections of THR123 (5 μg/g, i.p.), THR184 (5 μg/g, i.p.) or saline for two weeks, starting on day 15 after TAC, when the LV already exhibited some degree of hypertrophy and functional deterioration. As shown in Fig. 5, the administration of THR184 during the 3rd and 4th weeks of TAC prevented the progression of the LV hypertrophy, as determined echocardiographically (Fig. 5A & B), and halted the progression of systolic (MAPSE) and diastolic (E/e') dysfunction (Fig. 5C & D). Moreover, a paired comparison of the echocardiographic variables from the same subject at four vs. two weeks indicated that the 15 days treatment with THR184 promoted significant recovery of MAPSE and E/e', thus suggesting a reverse remodeling effect. Gravimetric analysis of the LV mass, harvested 4 weeks after TAC, showed a significant weight decrease only in those animals treated with THR184 compared to saline, which agrees with the echocardiographic analysis (Fig. S3).

In contrast, the beneficial effects of THR123 at the dose studied did not reach statistical significance, compared to TAC-saline mice, except for halting septal wall thickening and promoting a slight recovery of MAPSE (Fig. 5).

Treatment with THR184, starting on day 15 after TAC, significantly decreased the myocardial expression of *Col 1a1* and *β-MHC* compared with saline (Fig. 6A & B). The treatment with the peptides during the third and fourth weeks did not reduce the expression of *BNP* significantly compared with saline. However, in mice treated with THR184, the levels of *BNP* did not differ significantly from those of the sham mice (Fig. 6C). In addition, fibrosis quantification in histological sections stained with Masson's trichrome (Fig. 6D & E) showed less deposition of fibrillar elements into the ECM in THR184-treated mice. Furthermore, the average cardiomyocyte diameter was significantly smaller in the THR184-TAC group than in the TAC-saline group (Fig. 6F). Detailed cross sectional area of cardiomyocytes in mice LV sections are shown in Fig. S5B.

Together, the results revealed that the initiation of treatment with THR184 when pathological remodeling was already underway prevented the progression of structural damage and induced some degree of reverse remodeling, which attenuated the deleterious functional

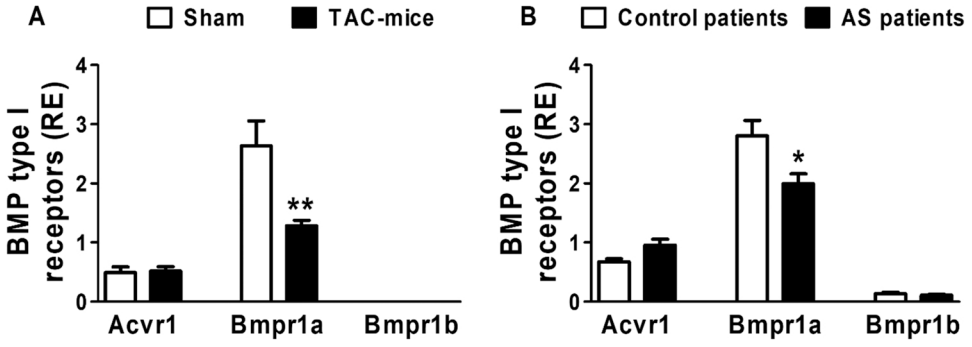

Fig. 2. Expression of BMP7 type I receptors in the LV from mice and AS patients: *Acvr1*, *Bmpr1a* and *Bmpr1b*. Relative mRNA expression was determined by qPCR and normalized to *18 S* (RE) in: (A) sham ($n = 6$) and TAC ($n = 7–9$) mice; (B) control ($n = 10$) and AS patients ($n = 33$). Data are expressed as means ± SEM. TAC vs. Sham mice: $^{**}p < 0.01$ (Student's t-test); AS patients vs. Control patients: $^{*}p < 0.05$ (Student's t-test). *Acvr1*, activin A receptor type 1; AS, aortic stenosis; *Bmpr1a*, bone morphogenetic protein receptor 1 A; *Bmpr1b*, bone morphogenetic protein receptor 1B; TAC, transverse aortic constriction.

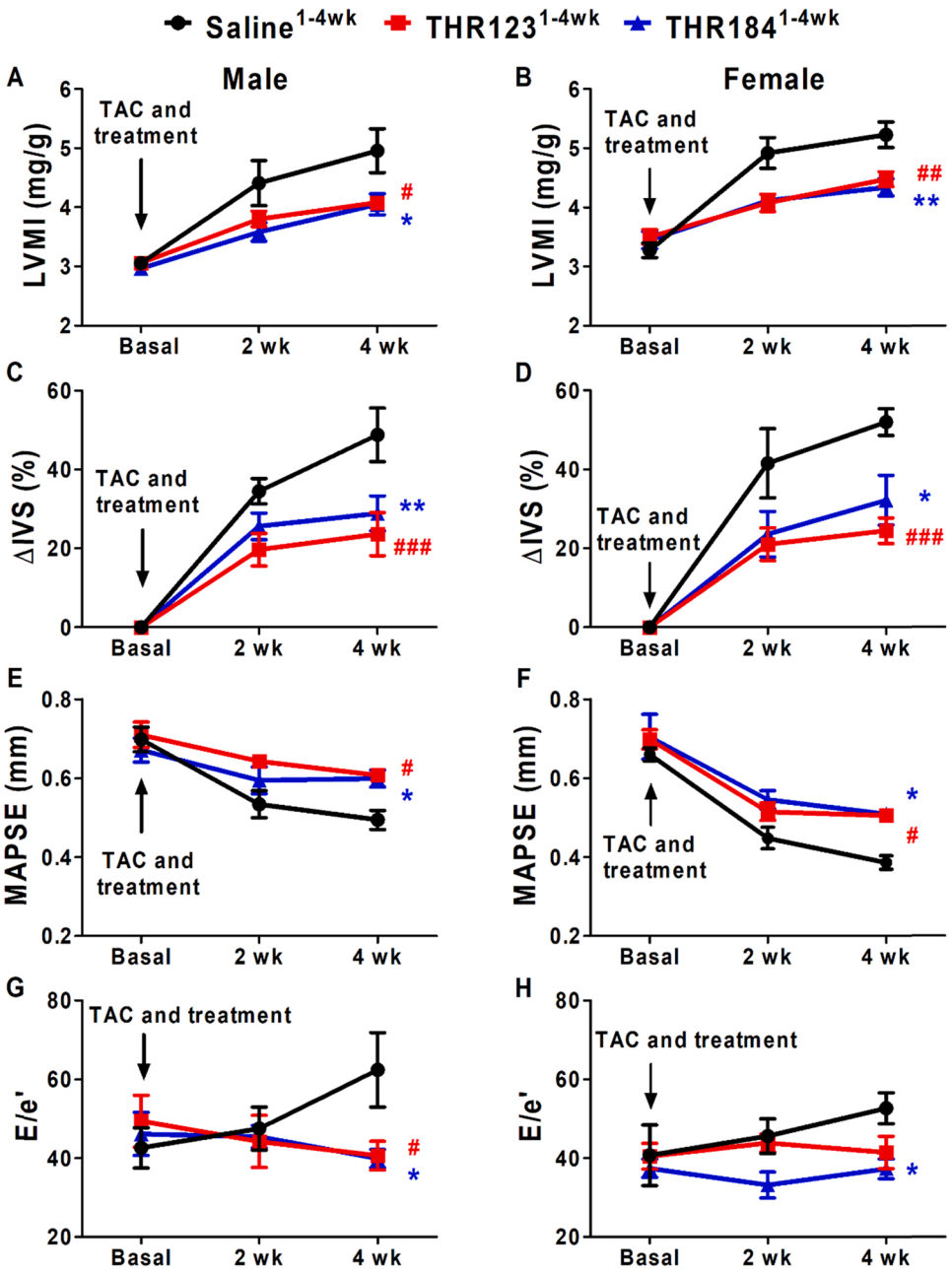

Fig. 3. Morphological and functional echocardiographic changes induced by pressure overload in male and female mice subjected to 4-week TAC. Mice received daily i.p. injections of saline (males, n = 10; females, n = 5), THR123 (males, n = 9; females, n = 7), or THR184 (males, n = 9; females, n = 8) during the 4 week follow-up period. (A & B) LVMI, LV mass indexed to body weight. (C & D) ΔIVS, increase of interventricular septum thickness. (E & F) MAPSE, mitral annular plane systolic excursion. (G & H) E/e', ratio of peak early transmitral flow velocity (E) to peak early myocardial tissue velocity (e'). Data are expressed as means ± SEM. THR123 vs. saline: #p < 0.05, ##p < 0.01, ###p < 0.001; THR184 vs. saline: *p < 0.05, **p < 0.01 (two-way ANOVA followed by Bonferroni post hoc test at 4 weeks).

consequences. In contrast, THR123, at the same dose, did not achieve such disease-modifying properties.

3.1.2.3. Effects of treatment with THR123 and THR184 on the expression of Bmpr1a and pSMAD1/5/(8)9 in the LV of TAC mice. We assessed whether the effects of THR123 and THR184 involved BMPR1A canonical SMAD-mediated signaling. First, we showed that the treatment with either peptide prevented *Bmpr1a* downregulation induced by TAC in the LV so that their expression recovered values similar to those of sham mice (Fig. 7A & B). Interestingly, the LV transcript levels of *Bmpr1a* from TAC-saline, TAC-THR123, and THR184 correlated directly with MAPSE, and inversely with the interventricular septum thickness, LVM, the posterior wall thickness, E/e', and the expression levels of *β-MHC* and *Col 1a1* which confirm the indirect cardioprotective role of *Bmpr1a* as we previously described [19] (Fig. S6).

Furthermore, mice subjected to 4-week TAC and treated with saline exhibited significantly lower LV expression of pSMAD1/5/(8)9 than did sham mice. In addition, treatment with either THR123 or THR184, compared with saline, prevented the downregulation of pSMAD1/5/(8)9 protein (Fig. 7C). On the other hand, when the treatment of TAC mice started on day 15 after TAC, only the group treated with THR184 showed significantly greater expression of pSMAD1/5/(8)9 than the saline group (Fig. 7D). These results are consistent with the effects of the peptides on LV structural and functional damage (Fig. 5).

3.1.2.4. Treatment with THR184 after releasing pressure overload. A series of mice were subjected to de-TAC surgery, four weeks after TAC. Since the treatment with THR184, starting on day 15 after TAC suggested a reverse remodeling effect, we evaluated this peptide to reverse the LV remodeling after pressure overload release. Firstly, we administrated the same dose of THR184 injected in the TAC animal studies (5 μg/g/day) during 7-day de-TAC period. However, no improvement in the reverse remodeling was observed (data not shown). Therefore, double dose was assessed (10 μg/g/day).

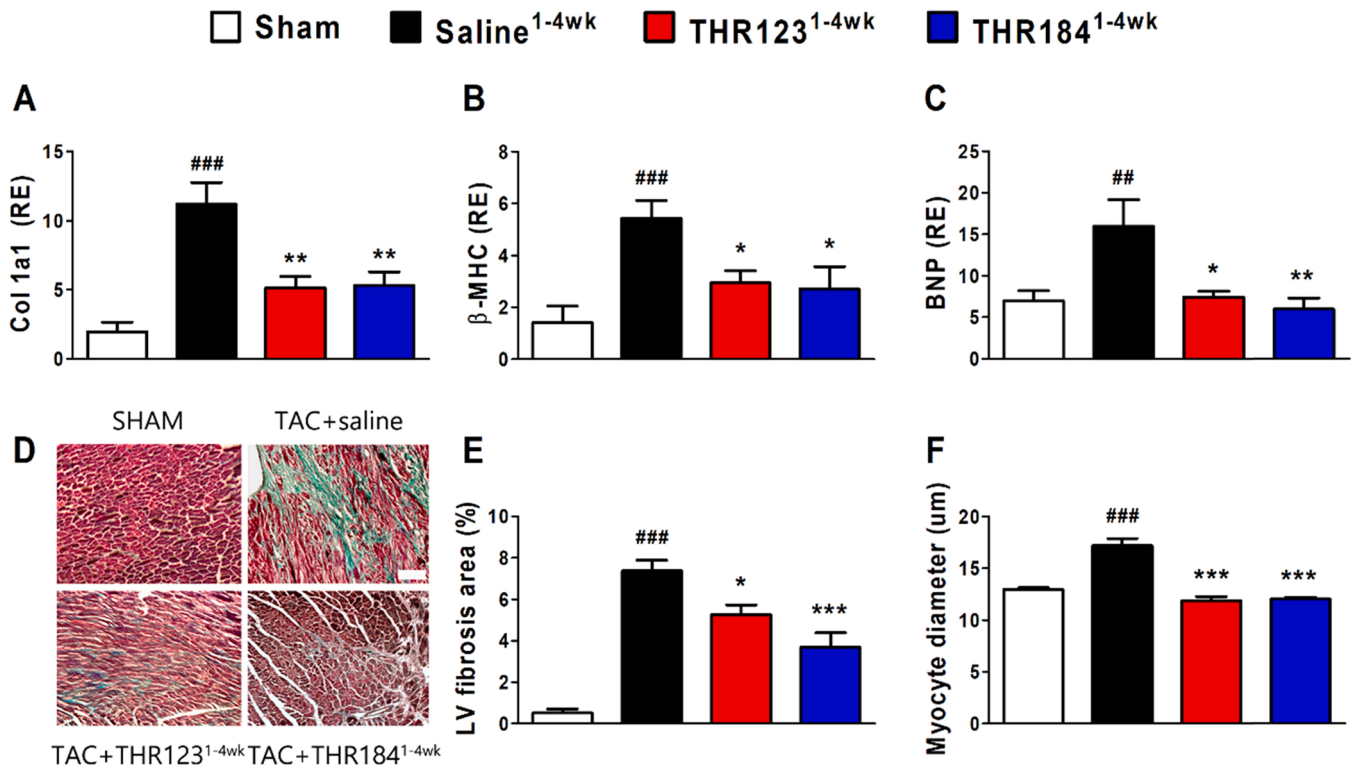

Fig. 4. Effects of the treatment with THR123 and THR184 during the entire TAC period on LV remodeling induced by pressure overload in mice. TAC mice were treated daily with saline, THR123, or THR184 during a 4-week follow-up. (A, B & C) Myocardial mRNA relative expression (RE, normalized to ribosomal *18S* RNA) of fibrosis (A: *Col 1a1*), hypertrophy (B: *β-MHC*) and heart failure (C: *BNP*) markers, in sham (n = 5–6), TAC+saline^{1-4wk} (n = 7), TAC+THR123^{1-4wk} (n = 6–7) and TAC+THR184^{1-4wk} (n = 6) mice. Data are expressed as mean ± SEM. TAC+saline^{1-4wk} vs. sham: ##p < 0.01; ###p < 0.001; TAC+THR123^{1-4wk} or TAC+THR184^{1-4wk} vs. TAC+saline^{1-4wk}: *p < 0.05; * *p < 0.01 (One-way ANOVA followed by Bonferroni's post hoc test). (D) Representative images of LV sections stained with Masson trichrome showing myocardial fibrosis in blue. Scale bar: 100 μm. (E) Percentage of fibrotic LV area in short-axis LV sections (3 sections per mouse, 3–6 mice per group). TAC+saline^{1-4wk} vs. sham: ###p < 0.001; TAC+THR123^{1-4wk} or TAC+THR184^{1-4wk} vs. TAC+saline^{1-4wk}: *p < 0.05, ***p < 0.001 (One-way ANOVA followed by Bonferroni's post hoc test). (F) Average diameter of cardiomyocytes determined in LV sections (4 sections per mouse, 3–6 mice per group). TAC+saline^{1-4wk} vs. sham: ###p < 0.001; TAC+saline^{1-4wk} vs. sham: ***p < 0.001 (One-way ANOVA followed by Bonferroni's post hoc test).

The percentage of LV mass loss one week after pressure overload release was significantly greater in mice treated with THR184 (Fig. 8A). Besides, THR184 favored the recovery of LV systolic and diastolic function, as shown the percentage of MAPSE recovery (Fig. 8B) and the parameter E/e' (Fig. 8C). All these data indicate a greater reverse remodeling and functional recovery in THR184-treated mice compared to the saline group.

3.2. Studies in vitro

3.2.1. Effects of THR123 and THR184 in cultured NIH-3T3 fibroblasts and H9C2 cardiomyocytes

The addition of THR123 and THR184 to the culture medium did not affect the viability and proliferation of NIH-3T3 fibroblasts and H9C2 cardiomyocytes (10^4 cells/well) in the MTS assays (Fig. S7).

NIH-3T3 fibroblasts and H9C2 cardiomyocytes were activated with TGF-β1 (10 ng/ml) to induce *Col 1a1* and *β-MHC* overexpression. Conversely, co-administration of TGF-β1 (10 ng/ml) with either THR123 or THR184 (1 μg/ml) resulted in repression of TGF-β1-induced transcriptional activation of the remodeling-related genes in both cell types (Fig. 9A & B). In addition, TGF-β1 induced the growth of H9C2 cardiomyocytes, whereas THR123 and THR184 attenuated TGF-β1-induced hypertrophy (Fig. S5C & D).

To determine which receptor is involved in the effects of THR123 and THR184, we tested two inhibitors with differential selectivity for each type I receptor: (i) DMH2 at 5 nM blocks BMPR1B and BMPR1A, but not ACVR1 (ii) LDN-193189 at 30 nM blocks BMPR1A and ACVR1, but not BMPR1B. As shown in Fig. 9, the inhibitory effects of both peptides on TGF-β1-induced transcriptional activation of *Col 1a1* in fibroblasts and *β-MHC* in cardiomyocytes were prevented by both antagonists. The antagonism by DMH2 at 5 nM ruled out the participation of ACVR1, and LDN-19318930 at 30 nM excluded BMPR1B mediated effects. Overall, these findings may support BMPR1A-mediated effects.

3.2.2. Effects of THR123 and THR184 on fibroblast proliferation, migration and phenotypic transformation into myofibroblasts promoted by TGF-β1

Under stress, fibroblasts undergo differentiation into highly specialized synthetic myofibroblasts, whose sustained activation results in excessive fibrosis and progressive LV dysfunction. TGF-β1 activates myofibroblast differentiation while BMP7 exerts the opposite effect [33]. Therefore, we assessed whether THR123 and THR184 might modulate the transdifferentiation of fibroblasts into myofibroblasts induced by TGF-β1.

In primary mouse cardiac fibroblasts, TGF-β1 increased the transcription of the coding gene (*Acta-2*) and the protein level of the myofibroblast marker α-SMA. Conversely, the addition of THR123 or THR184 to the medium decreased TGF-β1-induced *Acta-2* and α-SMA overexpression (Fig. 10A & B).

Immunofluorescence assays confirm that the stimulation of primary fibroblasts with TGF-β1 resulted in cytoskeletal reorganization and an increase in α-SMA expression. However, fibroblast co-treatment with TGF-β1 and either THR123 or THR184 prevented TGF-β1-induced formation of α-SMA filaments (Fig. 10C).

The fibrotic response was also characterized by assessing the proliferation and migration of primary cardiac fibroblasts induced by TGF-

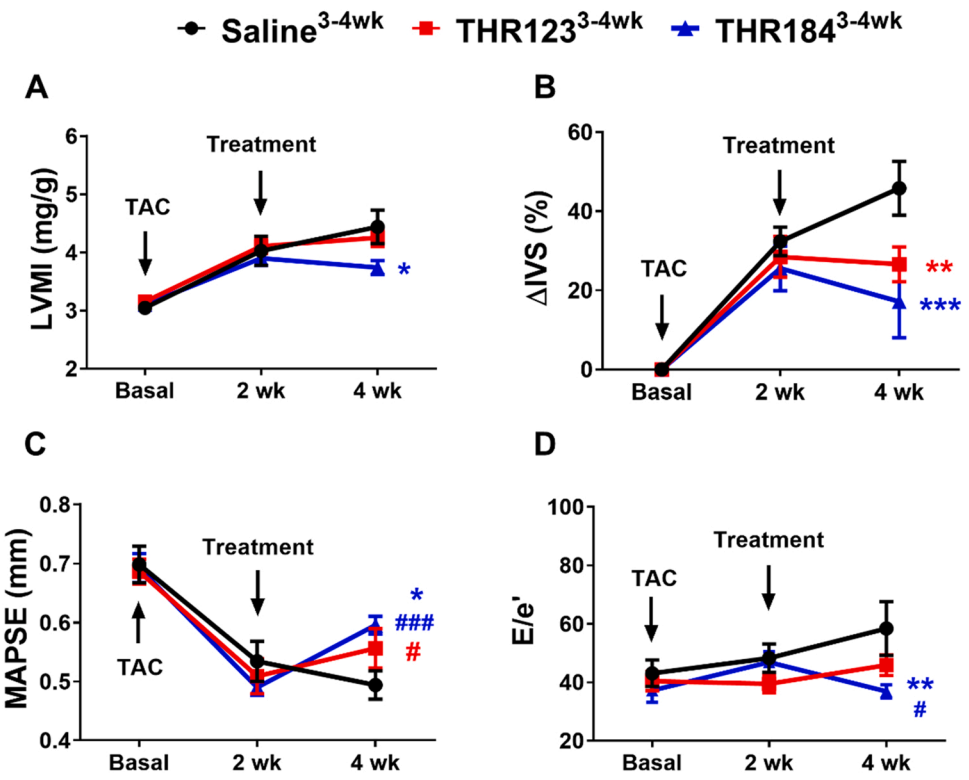

Fig. 5. Effects of the treatment with THR123 and THR184 during the 3rd and 4th weeks after TAC on morphological and functional echocardiographic parameters. TAC-mice were treated daily with saline (n = 10), THR123 (n = 9) and THR184 (n = 9), starting two weeks after TAC surgery. (A) LVMI, LV mass indexed to body weight. (B) ΔIVS, increment of interventricular septum thickness. (C) MAPSE, mitral annular plane systolic excursion. (D) E/e', ratio of peak early transmitral flow velocity (E) to peak early myocardial tissue velocity (e'). Data are expressed as means ± SEM. THR123 vs. saline: $^{**}p < 0.01$; THR184 vs. saline: $^{*}p < 0.05$, $^{**}p < 0.01$, $^{***}p < 0.001$ (two way ANOVA followed by Bonferroni post hoc test at four week-TAC). THR123 at 4 weeks vs. 2 weeks: $\#p < 0.05$; THR184 at 4 weeks vs. 2 weeks: $\#p < 0.05$, $\#\#\#p < 0.001$ (Student's paired t-test).

β1 [34]. Stimulation with TGF-β1 significantly increased fibroblast proliferation as indicated by BrdU incorporation. The proliferative response was prevented by THR123 or THR184 (Fig. 10D).

TGF-β1-induced migration of cardiac fibroblasts was assessed in wound healing assays. As shown in Fig. 10E & F, THR123 and THR184 attenuated cell migration.

Further, we determined *Acta-2* mRNA expression in the LV of TAC mice treated with THR123 or THR184 during the 4-week TAC period (Fig. 11A) or during the 3rd and 4th weeks post-TAC (Fig. 11B). Both treatment protocols significantly reduced *Acta-2* expression compared with saline. Our results support that THR123 and THR184 also decrease *in vivo* the transdifferentiation of fibroblasts into myofibroblasts.

3.3. Studies in silico

3.3.1. Binding interaction of THR123 and THR184 with the human BMPR1A receptor

The essential quantitative parameter that describes molecular interactions between biomolecules is binding affinity, which is often used as a proxy for drug potency *in vivo* [35,36] Radioligand-receptor binding assays [17] indicated the specific binding of THR123 to BMPR1A; however, they did not provide information on the binding affinity of the peptide to BMPR1A. To assess the hypothetical binding between the BMPR1A receptor and the peptides, and to determine whether large differences existed in this binding because of the 3D peptide structures, we performed molecular docking analysis to model the most likely interaction of THR123 and THR184 with the *Homo sapiens* BMPR1A receptor.

We selected the known human BMPR1A structure in its bound form, deposited in PDB under the accession number 2QJB. We used the bound form of the BMPR1A receptor for the docking studies, because this receptor has a highly flexible region associated with the binding of BMPs, and binding results in a disordered-to-ordered transition that generates an α-helix within the receptor binding site, which is not present in the free form of the receptor [37].

Regarding the peptides, we generated the 3D structures that were more energetically stable according to their amino acid sequence (Table S2). Both peptide sequences contain two cysteine residues that stabilize the cyclic structures of the peptides through a disulfide bond (Fig. 12D) [17].

In the molecular docking analysis, we selected binding models based on the interaction with Gln86 from the BMPR1A receptor. Gln86 is a highly conserved amino acid in BMPR1A that has been postulated to be essential for binding BMPs and is present in the region of BMPR1A associated with BMP binding [30].

The values that define the interaction of BMP7 with BMPR1A are shown in Table 1. The complex BMPR1A-BMP7 was energetically stable, as shown by the normalized stability of the complex.

The complexes of BMPR1A and either THR123 or THR184 exhibited similar normalized stability and binding energies (dG = complex energy – individual member energy) (Table 1). In addition, the values of normalized binding energy to SASA (Table 1) showed that the bindings of BMP7 or the peptides with BMPR1A were energetically similar.

Finally, we studied the interaction of THR123 or THR184 with the BMPR1A-BMP7 complex. The complexes BMPR1A-BMP7-peptide exhibited higher binding energies and lower SASA values than the complex BMPR1A-BMP7 (Table 1). These results indicated that both peptides alter the original interface topology in the BMPR1A-BMP7 complex (Fig. 12A, B & C), binding to the BMP binding region of BMPR1A, thus acting as competitive agonists.

4. Discussion

Detrimental remodeling of the LV, which can result from myocardial damage or hemodynamic stress, is a major cause of heart failure [1], for which effective mechanism-targeted therapies are not yet available. Recent preclinical investigations have demonstrated that endogenous and rhBMP7 protect the myocardium against maladaptive phenotypic plasticity in experimental models of clinically relevant heart diseases, which strongly suggest the cardioprotective therapeutic potential of BMP7-based approaches [11,19,22,38,39]. In this regard, peptide technology studies have identified several small BMP7-derived peptide

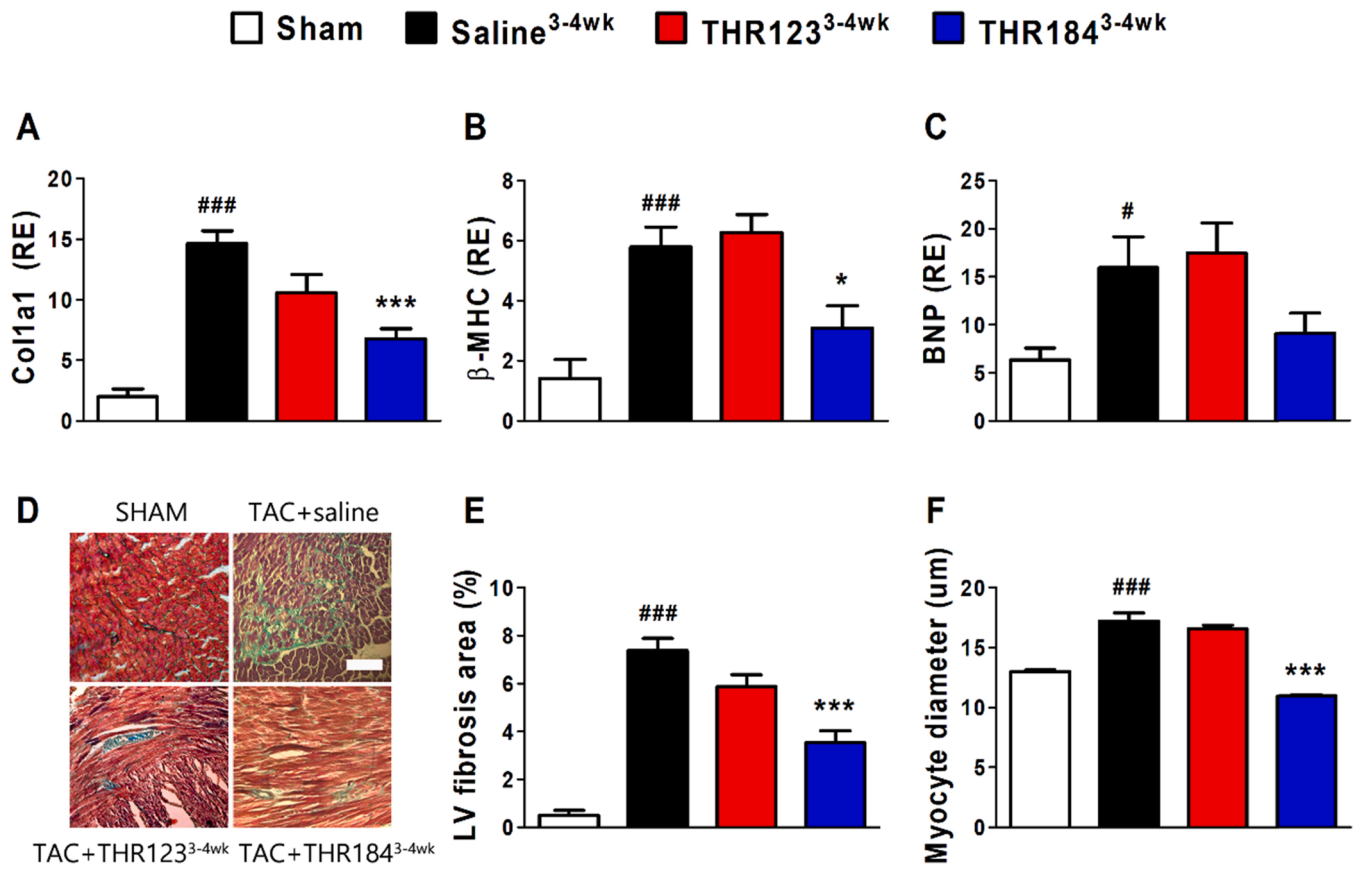

Fig. 6. Effects of the treatment with THR123 and THR184 during the 3rd and 4th weeks after TAC on the progression of myocardial structural remodeling. (A, B & C) Myocardial mRNA relative expression (RE, normalized to ribosomal *18S* RNA) of fibrotic (A: *Col 1a1*), hypertrophy (B: *β-MHC*) and heart failure (C: *BNP*) markers in sham (n=5-6), TAC-saline$^{3\text{-}4wk}$ (n=5-7), TAC-THR123$^{3\text{-}4wk}$ (n=5-6), and TAC-THR184$^{3\text{-}4wk}$ (n=6-7) mice. Data are expressed as means ± SEM. TAC-saline$^{3\text{-}4wk}$ vs. sham: #p < 0.05, ###p < 0.001; TAC-THR123$^{3\text{-}4wk}$ or TAC-THR184$^{3\text{-}4wk}$ vs. TAC-saline$^{3\text{-}4wk}$: *p < 0.001, ***p < 0.001 (One-way ANOVA followed by Bonferroni's post hoc test). (D) Representative images of LV sections stained with Masson trichrome showing myocardial fibrosis in blue. Scale bar: 100 μm. (E) Percentage of fibrotic LV area in short-axis LV sections (3 sections per mouse, 3 to 6 mice per group). TAC-saline$^{3\text{-}4wk}$ vs. sham: ###p < 0.001; TAC-THR123$^{3\text{-}4wk}$ or TAC-THR184$^{3\text{-}4wk}$ vs. TAC-saline$^{3\text{-}4wk}$: ***p <0.001 (One-way ANOVA followed by Bonferroni's post hoc test). (F) Average cardiomyocyte diameter determined in LV sections (4 sections per mouse, 3 to 6 mice per group). TAC-saline$^{3\text{-}4wk}$ vs. sham: ###p < 0.001; TAC-saline$^{3\text{-}4wk}$ vs. sham: ***p <0.001 (One-way ANOVA followed by Bonferroni's post hoc test).

sequences, including THR123 and THR184, with favorable biological activities *in vitro* and *in vivo* models of renal fibrosis [17,26]. Direct evidence on the involvement of BMPR1A in the renoprotective activity of THR123 is provided by its targeted deletion in the renal tubular epithelium [17].

The cell-type differential bioactivity of BMPs is dependent on the receptors expressed [40]. Therefore, we first explored whether BMPR1A signaling may be involved in the cardioprotective effects of BMP7. Herein, we show that *Bmpr1a* was the most abundantly expressed receptor in the healthy LV myocardium in humans and mice; on the other hand, *Acvr1* was scarcely expressed, and *Bmpr1b* was virtually absent.

Bmpr1a downregulation in the LV of patients with AS and TAC-mice is congruent with the maladaptive dysregulation of fibrosis homeostasis towards impairing BMP7 antifibrotic signaling, previously described in the pressure overload condition [19].

On the other hand, *Acvr1* overexpression positively correlated with LV hypertrophy in TAC mice (r = 0.77*) and AS patients (r = 0.32*), which is consistent with the involvement of ACVR1 signaling in cardiomyocyte hypertrophy induced *in vitro* by phenylephrine, and *in vivo* by angiotensin II in mice [41].

Overall, these results support that pharmacological restoration of canonical BMP7 signaling through BMPR1A receptors via treatment with agonist drugs may counteract the forces driving maladaptive phenotypic changes in the afterload-stressed myocardium.

In the present study, we established the cardioprotective effects of two BMP7-based Sugimoto's peptides, THR123 and THR184, in mice of either sex subjected to TAC. Daily i.p. injection of either peptide during four weeks, starting on the day of TAC surgery, (i) rescued the expression of *Bmpr1a* and associated pSMAD1/5/(8)9 signaling in the LV, (ii) prevented transcriptional activation of remodeling-associated genes (*Col 1a1*, *β-MHC*, *BNP* and *Acta-2*), (iii) attenuated LV structural damage (hypertrophy and fibrosis), and (iv) diminished LV dysfunction (systolic and diastolic).

In the context of LV under pressure overload, although a large body of evidence supports that TGF-βs are essential drivers of fibrosis and hypertrophy remodeling programs [13,42,43], the pathophysiological importance of a dysfunctional counterbalance by BMP7 is incompletely understood [19,20,44]. Our previous findings in patients with AS and TAC mice have revealed that lower myocardial expression of BMP7 is associated with higher TGF-β signaling, more severe structural damage in terms of fibrosis and hypertrophy, and more significant functional echocardiographic abnormalities, thus supporting the imbalance between opposing BMP7 and TGF-β signals. In addition, *in vitro* assays indicated that rhBMP7 prevents TGF-β-induced transcriptional activation of *Col 1a1* in fibroblasts and inhibits the ability of TGF-β to activate the hypertrophic transcription program in cardiomyocytes [19].

In vitro bioactivity assays revealed the counteracting effects of THR123 and THR184 against TGF-β1-induced overexpression of *Col 1a1*

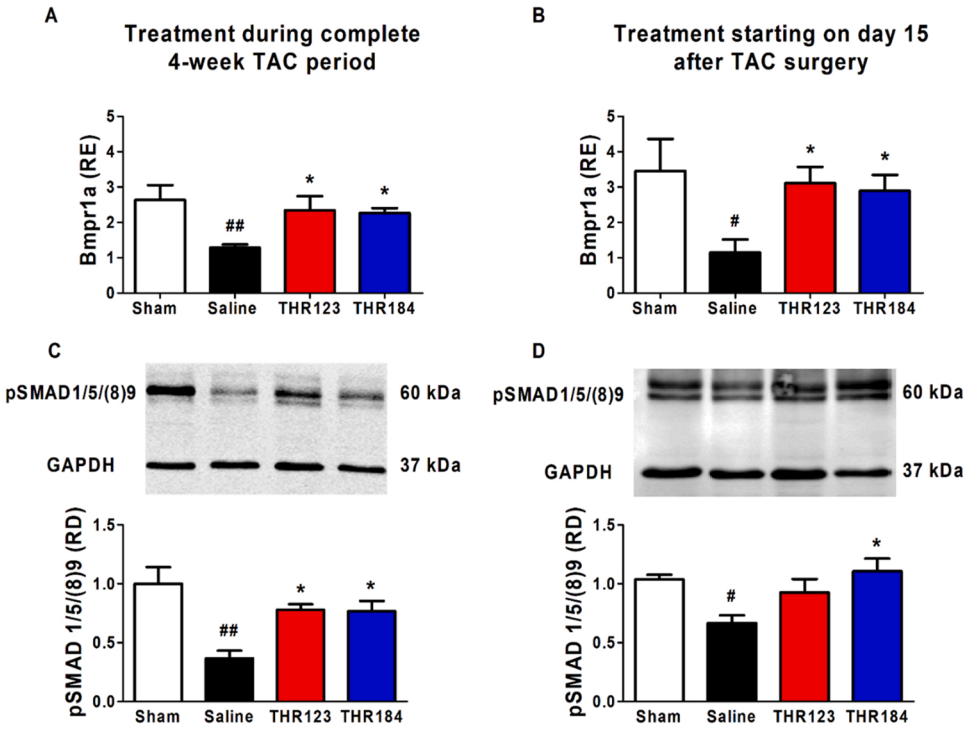

Fig. 7. Gene expression of *Bmpr1a* and protein levels of pSMAD1/5/(8)9 determined in LV samples. (A & B) Myocardial mRNA relative expression [sham (n = 6), TAC-saline (n = 8), TAC-THR123 (n = 7), and TAC-THR184 (n = 7)] and (C & D) representative blots from mice (n = 3 per group) treated during the entire 4-week TAC period (A & C) and mice that received the treatment during the 3rd and 4th weeks after TAC (B & D). Data are expressed as means ± SEM of the relative expression (RE, normalized to ribosomal *18S* RNA) or relative optical density (RD vs. GAPDH). TAC-saline vs. Sham: #p < 0.05, ##p < 0.01; TAC-THR123 or TAC-THR184 vs. TAC-saline: *p < 0.05 (One-way ANOVA followed by Bonferroni's test).

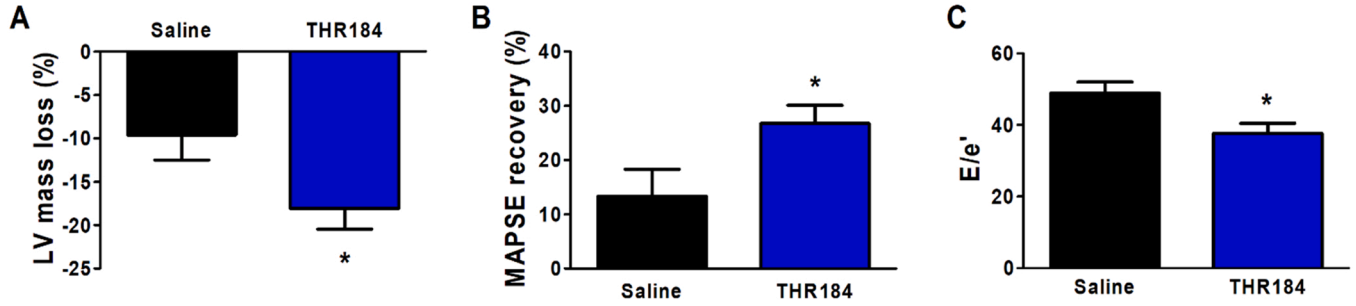

Fig. 8. THR184 effects on reverse remodeling after TAC release. Mice were treated with saline (n = 7) or THR184 (n = 7), during 7 days after de-TAC surgery. (A) LV mass loss, left ventricle mass loss. (B) MAPSE recovery, mitral annular plane systolic excursion. (C) E/e', ratio of peak early transmitral flow velocity (E) to peak early myocardial tissue velocity (e'). Data are expressed as means ± SEM. THR184 vs. saline: *p < 0.05 (Student's t-test).

in NIH-3T3 fibroblasts and *β-MHC* in H9C2 cardiomyocytes, as well as the involvement of BMPR1A. Moreover, in primary cultures of mouse cardiac fibroblasts, we observed that THR123 and THR184 attenuated the TGF-β1-induced cardiac fibroblast proliferation and migration and the overexpression of the contractile protein α-SMA and its coding gene *Acta-2*, which are markers of myofibroblast phenotypic activation. Accordingly, the LV in TAC mice treated with THR123 and THR184 exhibited a significant decrease in *Acta-2* expression. Myofibroblasts are contractile fibroblasts that produce large amounts of fibrotic extracellular matrix (ECM) molecules, whose pathological activation and persistence within tissues correlate with the progression of fibrotic diseases [45,46]. TGF-β1 is considered the primary driver of fibroblast-to-myofibroblast transdifferentiation.

Furthermore, a recent report has shown that BMP7 canonical SMAD signaling prevents the TGF-β1-induced transdifferentiation of human lung fibroblasts into myofibroblasts [29]. Interestingly, the potential reversibility of the myofibroblast phenotype has been demonstrated in cultured myofibroblasts isolated from human end-stage failing hearts through inhibition of TGF-β1 signaling [47]. The implication that cardiac myofibroblasts retain the ability to return to a less activated state provides further insights into the potential of myofibroblast-targeted BMP7-based therapies to delay and/or reverse the progression of LV fibrosis.

The antihypertrophic role of BMPR1A signaling is supported by several pieces of evidence from our studies *in vivo* and *in vitro*. (i) In TAC mice, pharmacological activation of BMPR1A signaling with its selective agonists THR123 and THR184 effectively prevented, halted, and/or reversed LV hypertrophy, as reflected by the evolution of LV myocyte diameter, LV wall thicknesses and LV mass. (ii) The treatment of mice with THR184 after releasing the pressure overload by de-TAC surgery significantly augmented cardiac mass loss in the context of reverse remodeling. (iii) In both AS patients and TAC mice, the LV expression of *Bmpr1a* exhibited an inverse relationship with LV wall thicknesses and LV mass and the transcript levels of the hypertrophy marker *β-MHC*. (iv) In cultured H9C2 cardiomyocytes, THR123 and THR184 prevented TGF-β1-induced hypertrophy.

The clinical diagnosis of valvular aortic stenosis commonly occurs after long periods of silent but progressive increases in LV hemodynamic stress. Thus, most patients exhibit some degree of LV remodeling when they are referred for treatment. However, effective pharmacological therapies to delay or reverse remodeling are yet lacking. After patients develop symptoms, the only effective treatment currently available is

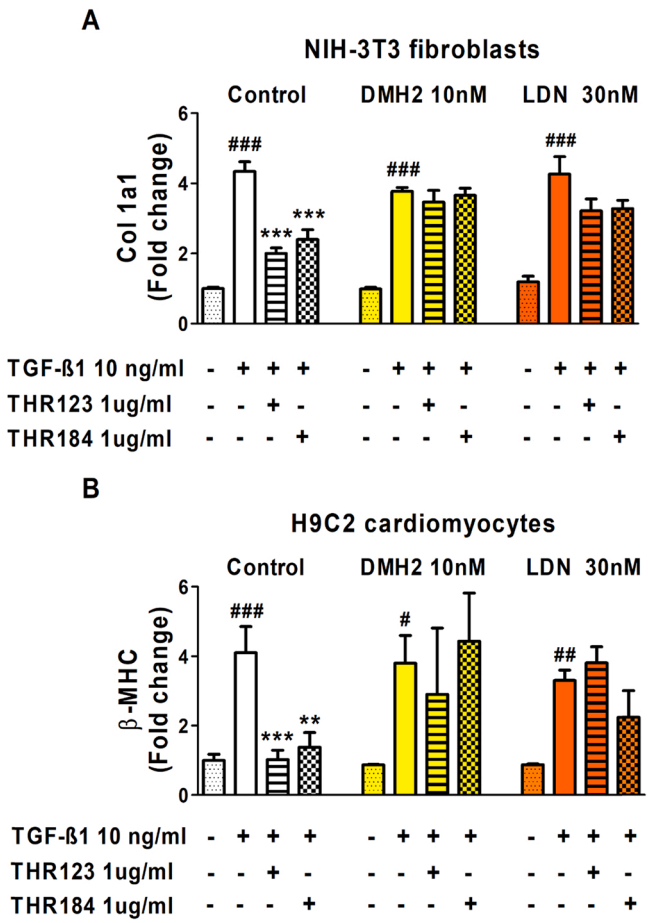

Fig. 9. Inhibition of BMP type I receptors in treated cell lines with THR123 or THR184. (A & B) mRNA relative expression (RE) levels of *Col 1a1* (A) and *β-MHC* (B) related to housekeeping *18 S* in NIH-3T3 fibroblasts (A) and H9C2 cardiomyocytes (B) incubated overnight with DMH2 10 nM or LDN-193189 30 nM, two BMP type I receptor inhibitors. Then, TGF-β1 (10 ng/ml), and THR123 (1 μg/ml) or THR184 (1 μg/ml) were added to stimulate cells and evaluate the effects of BMP receptor inhibitors in the expression of *Col 1a1* and *β-MHC*. TGF-β1 vs. Control: ###$p < 0.001$; TGF-β1 + THR123 or TGF-β1 + THR184 vs. TGF-β1: **$p < 0.01$, ***$p < 0.001$; DMH2 +TGF-β1 vs. DMH2: #$p < 0.05$, ###$p < 0.001$; LDN+TGF-β1 vs. LDN: ##$p < 0.01$, ###$p < 0.001$ (One-way ANOVA followed by Bonferroni's test).

open surgical or transcatheter aortic valve replacement [4,48,49]. Interestingly, we observed the most striking results with peptide treatment beginning two weeks after surgery, a time at which the remodeling process was in progress, and LV hypertrophy and functional deterioration were already ongoing. In this realistic context, THR184 restored the control values of *Bmpr1a* and pSMAD1/5/(8)9, attenuated the transcriptional activation of remodeling-associated genes, and halted the LV structural damage and systolic and diastolic dysfunction. Furthermore, THR184 promoted some recovery in the echocardiographic parameters of systolic (MAPSE) and diastolic (E/e') functions, thus suggesting reverse remodeling. Regarding the clinical interest, exogenous administration of THR184 plays a relevant positive role in the reverse remodeling process after releasing pressure overload. Treatment of mice with THR-184 during one week after de-TAC improved some features of the reverse remodeling. Remarkably, hypertrophy and LV longitudinal systolic and diastolic function were significantly improved during the de-TAC recovery period.

Unexpectedly, THR123 administered with the same schedule as THR184 during the 3rd and 4th weeks of TAC did not demonstrate such favorable disease-modifying properties and only partially recovered some transcriptional and functional maladaptive changes.

The lack of bioactivity differences *in vitro* between THR123 and THR184 in cultured fibroblasts and cardiomyocytes does not explain the worse *in vivo* beneficial effect exhibited by THR123 vs. THR184 in TAC mice. Therefore, we assessed whether these discrepant findings might be associated with potential receptor binding differences derived from the particular 3D structure of each peptide. The specific but weak binding of THR123 to the extracellular domain of BMPR1A has been reported previously by Sugimoto et al. in radioligand competitive binding assays [17]. However, the study does not provide data on the binding affinities of THR184 nor other molecules of the same series that allow us to infer potential differences in the pharmacological potency of THR123 and THR184 *in vivo*. Herein, we *in silico* modeled the hypothetical interaction of THR123 and THR184 with the human BMPR1A receptor by using molecular docking analyses. Our bioinformatics data predicted that BMP7 and both peptides form energetically stable complexes with the BMPR1A receptor. The interaction of THR123 and THR184 with the BMPR1A-BMP7 complex increased the binding energy and decreased the solvent-accessible surface area of BMP7 binding to BMPR1A. These results indicate that both peptides interacted with the BMP binding domain of BMPR1A to alter the binding interface between BMP7 and BMPR1A. The similarity of the binding energies suggests that both peptides exhibit comparable affinity for the receptor; therefore, even with the limitations of an *in silico* study, a similar pharmacological potency would be expected for both agonists.

There are inevitable limitations in our study. TAC mice are the most common experimental model of pressure overload but present substantial differences with the clinical scenario which limits the direct extrapolation of preclinical experiments into clinical practice. One of the principal differences in TAC model is the immediate onset of pressure overload, in contrast to the slow progression of aortic valve stenosis in patients. Therefore, any treatment assessed in TAC or de-TAC animal models against cardiac remodeling must be interpreted with caution.

In conclusion, the present study supports that impaired BMP7 signaling through BMPR1A receptors in the LV is a relevant feature of the maladaptive remodeling developed in response to pressure overload stress in experimental settings (transverse aortic constriction in mice) and clinical settings (aortic stenosis patients). Furthermore, our results in TAC mice demonstrate that the BMP7-based peptides THR123 and THR184 activated BMPR1A canonical pSMAD1/5/(8)9 signaling, thereby protecting against the structural damage and subsequent dysfunction of the LV induced by the hemodynamic burden. We show that the bioactivity of these peptides *in vitro* attenuated the phenotypic changes induced by TGF-β1 in fibroblasts (fibrogenesis) and cardiomyocytes (hypertrophy), which are important events underlying pathological cardiac remodeling. The present study results provide a preclinical proof-of-concept of potential therapeutic benefits of BMP7-based small peptides, which function as agonists of BMPR1A, against the deleterious consequences of LV pressure overload. Our observations may provide new insights aimed at promoting BMP7 signaling as a therapeutic target for the palliative treatment of LV remodeling in the aortic stenosis scenario. These findings may be important, given that aortic valve replacement is currently the only effective treatment for symptomatic patients with AS, and no pharmacologic tools are available to attenuate or reverse the adverse LV remodeling process.

Funding

This work was supported by grants from: Ministerio de Economía y Competitividad [(PI18/00543); CIBERCV (CB16/11/00264), co-funded by Fondo Europeo de Desarrollo Regional (FEDER)]; Instituto de Investigación Sanitaria Marqués de Valdecilla (IDIVAL) (INNVAL2018/20); Grants4Targets from BAYER AG (ID 2017-03-2088). A.B.S-M. received a pre-doctoral fellowship from IDIVAL (PREVAL18/03).

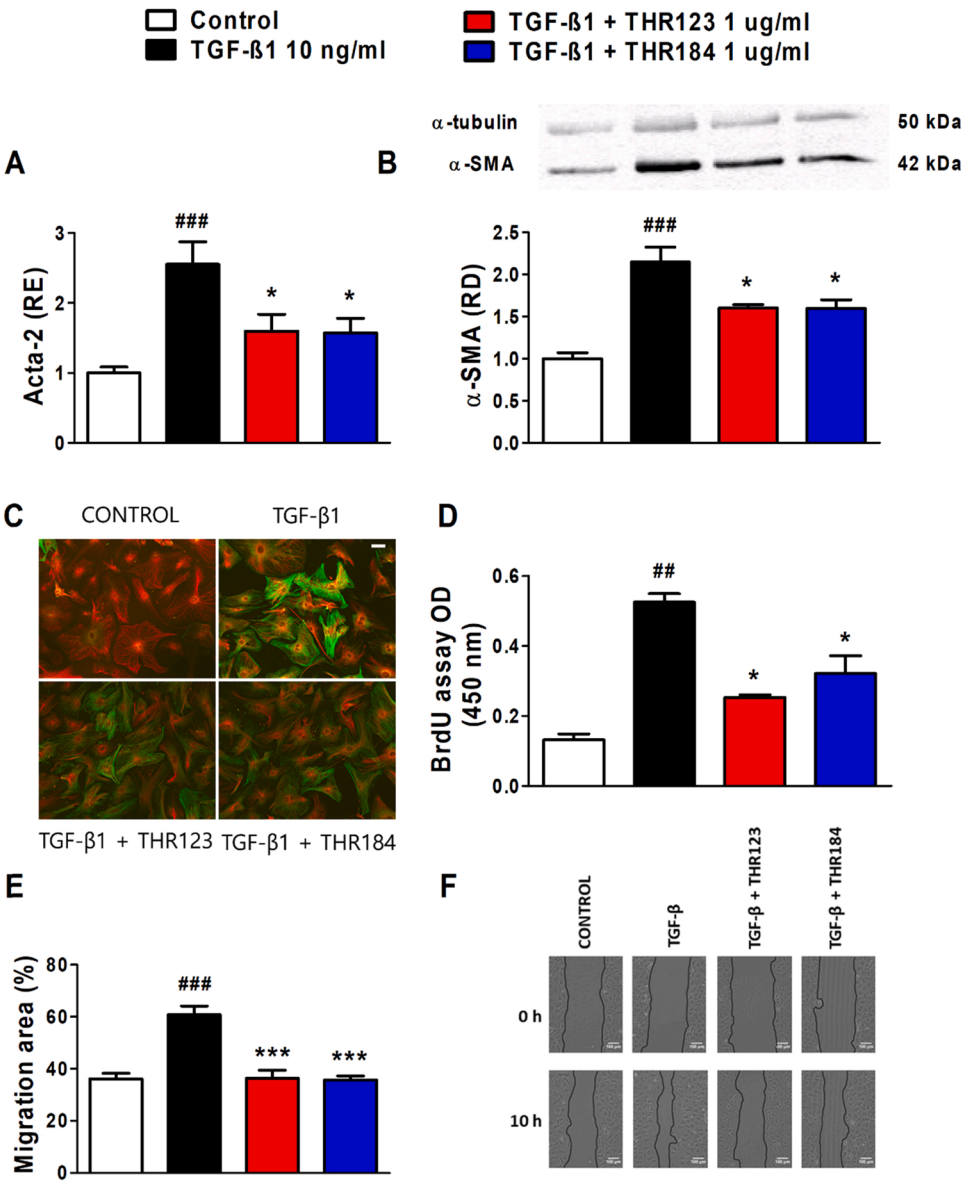

Fig. 10. Effects of THR123 and THR184 on transdifferentiation of cardiac fibroblasts into myofibroblasts. (A) mRNA relative expression (RE, normalized to ribosomal *18S* RNA) of *Acta-2* in primary cardiac fibroblasts treated with TGF-β1, TGF-β1 + THR123, and TGF-β1 + THR184 (n = 3 per group). Data are expressed as mean ± SEM. TGF-β1 vs. Control: ###p < 0.001; TGF-β1 + THR123 or TGF-β1 + THR184 vs. TGF-β1: *p < 0.05 (One-way ANOVA followed by Bonferroni's test). (B) Protein levels of α-SMA were determined by western blot in primary cardiac fibroblasts (n = 3 per group). Data are expressed as relative optical density (RD) vs. α-tubulin. TGF-β1 vs. Control: ###p < 0.001; TGF-β1 + THR123 or TGF-β1 + THR184 vs. TGF-β1: *p < 0.05 (One-way ANOVA followed by Bonferroni's test). (C) Representative IF of cardiac fibroblasts stained with α-SMA (green) and vimentin (red). Scale bar: 20 μm. (D) BrdU proliferation assay in primary cardiac fibroblasts. TGF-β1 vs. Control: ##p < 0.01; TGF-β1 + THR123 or TGF-β1 + THR184 vs. TGF-β1: *p < 0.05 (One-way ANOVA followed by Bonferroni's test). (E) Percentage of migration area of primary cardiac fibroblasts in wound healing assays. TGF-β1 vs. Control: ###p < 0.001; TGF-β1 + THR123 or TGF-β1 + THR184 vs. TGF-β1: ***p < 0.001 (One-way ANOVA followed by Bonferroni's test). (F) Representative images of cardiac fibroblasts in the wound healing assay. Scale bar: 100 μm.

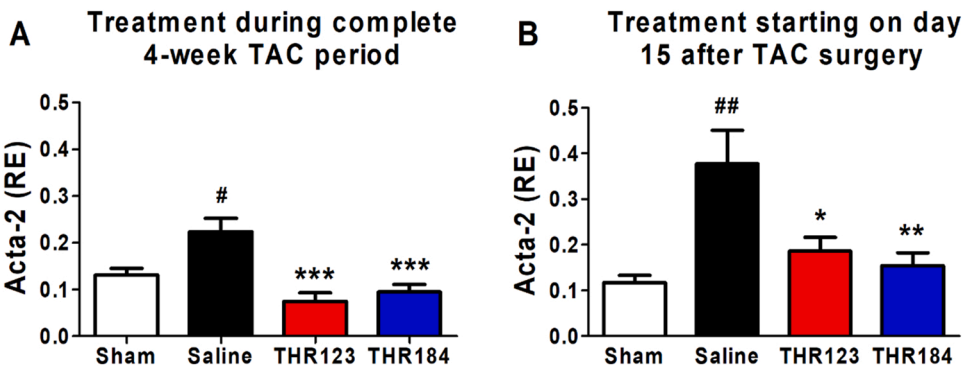

Fig. 11. Effects of THR123 and THR184 on *Acta-2* myocardial expression. (A & B) mRNA relative expression (RE, normalized to ribosomal *18S* RNA) of *Acta-2* in the LV from mice treated THR123 or THR184 during the whole 4-week TAC period (A) or the 3rd and 4th weeks after TAC (B). Data are expressed as means ± SEM. TAC-saline vs. Sham: #p < 0.05, ##p < 0.01; TAC-THR123 or TAC-THR184 vs. TAC-saline: *p < 0.05, * *p < 0.01, ***p < 0.001 (One-way ANOVA and Bonferroni's test).

CRediT authorship contribution statement

Ana B Salido-Medina: Conceptualization, Methodology, Formal analysis, Investigation, Data Curation, Writing-Original draft, Visualization. **Aritz Gil**: Methodology, Investigation, Resources. **Víctor Expósito**: Investigation, Resources. **Fernando Martínez**: Methodology, Formal analysis, Validation, Visualization, Writing – review & editing. **Juan M Redondo**: Writing-Review and Editing, Visualization. **María A Hurlé**: Conceptualization, Resources, Writing-Review and Editing, Visualization, Supervision. **J Francisco Nistal**: Conceptualization,

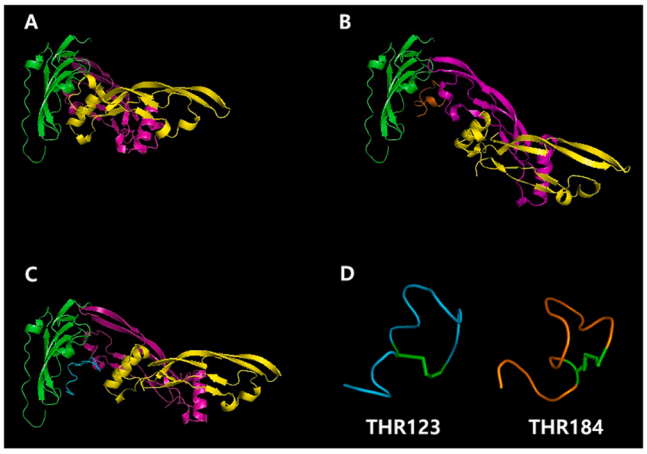

Fig. 12. Tridimensional representation of the different molecular complexes. Predicted binding between human BMPR1A receptor and the BMP7 dimeric cytokine (A; yellow and fuchsia), THR184 (B; orange) or THR123 (C; blue). All the models were structurally aligned to BMPR1A. (D) Three-dimensional representation of THR123 and THR184. Disulfide bonds are represented in green sticks between Cys1-Cys11 of each peptide.

Table 1
Energetic values of the different complexes after applying docking tools and Interface Analyzer software.

COMPLEX	NORMALIZED STABILITY OF COMPLEX (REU)	BINDING ENERGY (REU)*	SASA (Å^2)	NORMALIZED BINDING ENERGIES#
BMPR1A-BMP7	-2.214	-25.107	1809.125	-1.388
BMPR1A-THR123	-2.108	-15.809	1129.606	-1.286
BMPR1A-THR184	-2.146	-14.065	881.253	-1.596
BMPR1A-BMP7-THR123	-2.187	-12.389	1193.016	-1.038
BMPR1A-BMP7-THR184	-2.160	-10.246	1036.19	-0.989

REU: Rosetta Energy Units. SASA: Solvent Accessible Surface Area. *Binding energy → dG = complex energy – individual member energy. #Normalized binding energy → (binding energy/SASA) * 100.

Resources, Writing-Review and Editing, Visualization, Supervision, Funding acquisition. **Raquel García**: Conceptualization, Validation, Formal analysis, Writing- Original draft, Visualization, Supervision, Project administration, Funding acquisition.

Conflict of interest statement

The authors declare that there are no competing interests associated with the manuscript.

Acknowledgments

We acknowledge the excellent technical assistance of Nieves García-Iglesias, Ana Cayón, Roberto Moreta, and Abraham Velasco.

Appendix A. Supporting information

Supplementary data associated with this article can be found in the online version at doi:10.1016/j.biopha.2022.112910.

References

[1] B.R. Lindman, M.A. Clavel, P. Mathieu, B. Iung, P. Lancellotti, C.M. Otto, P. Pibarot, Calcific aortic stenosis, Nat. Rev. Dis. Prim. 2 (2016) 16006, https://doi.org/10.1038/nrdp.2016.6.
[2] J.S. Burchfield, M. Xie, J.A. Hill, Pathological ventricular remodeling: Mechanisms: Part 1 of 2, Circulation 128 (2013) 388–400, https://doi.org/10.1161/CIRCULATIONAHA.113.001878.
[3] W.M. Torres, S.C. Barlow, A. Moore, L.A. Freeburg, A. Hoenes, H. Doviak, M. R. Zile, T. Shazly, F.G. Spinale, Changes in myocardial microstructure and mechanics with progressive left ventricular pressure overload, JACC Basic Transl. Sci. 5 (2020) 463–480, https://doi.org/10.1016/j.jacbts.2020.02.007.
[4] C.M. Otto, R.A. Nishimura, R.O. Bonow, B.A. Carabello, J.P. Erwin, F. Gentile, H. Jneid, E.V. Krieger, M. Mack, C. McLeod, P.T. O'Gara, V.H. Rigolin, T.M. Sundt, A. Thompson, C. Toly, ACC/AHA guideline for the management of patients with valvular heart disease: a report of the American College of Cardiology/American Heart Association joint committee on clinical practice guidelines, Circulation 2021 (143) (2020) e72–e227, https://doi.org/10.1161/CIR.0000000000000932.
[5] J.M. Beach, T. Mihaljevic, J. Rajeswaran, T. Marwick, S.T. Edwards, E.R. Nowicki, J. Thomas, L.G. Svensson, B. Griffin, A.M. Gillinov, E.H. Blackstone, Ventricular hypertrophy and left atrial dilatation persist and are associated with reduced survival after valve replacement for aortic stenosis, J. Thorac. Cardiovasc. Surg. 147 (2014) 362–369, https://doi.org/10.1016/j.jtcvs.2012.12.016.
[6] M. Puls, B.E. Beuthner, R. Topci, A. Vogelgesang, A. Bleckmann, M. Sitte, T. Lange, S.J. Backhaus, A. Schuster, T. Seidler, I. Kutschka, K. Toischer, E.M. Zeisberg, C. Jacobshagen, G. Hasenfuß, Impact of myocardial fibrosis on left ventricular remodeling, recovery, and outcome after transcatheter aortic valve implantation in different haemodynamic subtypes of severe aortic stenosis, Eur. Heart J. 41 (2020) 1903–1914, https://doi.org/10.1093/eurheartj/ehaa033.
[7] J.W. Lowery, V. Rosen, Bone morphogenetic protein-based therapeutic approaches, Cold Spring Harb. Perspect. Biol. 10 (2018) a022327, https://doi.org/10.1101/cshperspect.a022327.
[8] C.J. David, J. Massagué, Contextual determinants of TGFβ action in development, immunity and cancer, Nat. Rev. Mol. Cell Biol. 19 (2018) 419–435, https://doi.org/10.1038/s41580-018-0007-0.
[9] F. Dituri, C. Cossu, S. Mancarella, G. Giannelli, The interactivity between TGFβ and BMP signaling in organogenesis, fibrosis, and cancer, Cells 8 (2019) 1130, https://doi.org/10.3390/cells8101130.
[10] E.H. Budi, J.R. Schaub, M. Decaris, S. Turner, R. Derynck, TGF-beta as a driver of fibrosis: physiological roles and therapeutic opportunities, J. Pathol. 254 (2021) 358–373, https://doi.org/10.1002/path.5680.
[11] E.M. Zeisberg, O. Tarnavski, M. Zeisberg, A.L. Dorfman, J.R. Mcmullen, E. Gustafsson, A. Chandraker, X. Yuan, W.T. Pu, A.B. Roberts, E.G. Neilson, M. H. Sayegh, S. Izumo, R. Kalluri, Endothelial-to-mesenchymal transition contributes to cardiac fibrosis, Nat. Med. 13 (2007) 952–961, https://doi.org/10.1038/nm1613.
[12] A.V. Villar, M. Cobo, M. Llano, C. Montalvo, F. González-Vílchez, R. Martín-Durán, M.A. Hurlé, J.F. Nistal, Plasma levels of transforming growth factor-β1 reflect left ventricular remodeling in aortic stenosis, PLoS One 4 (2009), e8476, https://doi.org/10.1371/journal.pone.0008476.
[13] N. Koitabashi, T. Danner, A.L. Zaiman, Y.M. Pinto, J. Rowell, J. Mankowski, D. Zhang, T. Nakamura, E. Takimoto, D.A. Kass, Pivotal role of cardiomyocyte TGF-β signaling in the murine pathological response to sustained pressure overload, J. Clin. Investig. 121 (2011) 2301–2312, https://doi.org/10.1172/JCI44824.
[14] A.V. Villar, R. García, M. Llano, M. Cobo, D. Merino, A. Lantero, M. Tramullas, J. M. Hurlé, M.A. Hurlé, J.F. Nistal, BAMBI (BMP and activin membrane-bound inhibitor) protects the murine heart from pressure-overload biomechanical stress by restraining TGF-β signaling, Biochim. Biophys. Acta 1832 (2013) 323–335, https://doi.org/10.1016/j.bbadis.2012.11.007.
[15] N.G. Frangogiannis, Cardiac fibrosis, Cardiovasc. Res. 117 (2021) 1450–1488, https://doi.org/10.1093/cvr/cvaa324.
[16] M. Zeisberg, J.I. Hanai, H. Sugimoto, T. Mammoto, D. Charytan, F. Strutz, R. Kalluri, BMP-7 counteracts TGF-β1-induced epithelial-to-mesenchymal transition and reverses chronic renal injury, Nat. Med. 9 (2003) 964–968, https://doi.org/10.1038/nm888.
[17] H. Sugimoto, V.S. LeBleu, D. Bosukonda, P. Keck, G. Taduri, W. Bechtel, H. Okada, W. Carlson, P. Bey, M. Rusckowski, B. Tampe, D. Tampe, K. Kanasaki, M. Zeisberg, R. Kalluri, Activin-like kinase 3 is important for kidney regeneration and reversal of fibrosis, Nat. Med. 18 (2012) 396–404, https://doi.org/10.1038/nm.2629.
[18] D. Liang, Y. Wang, Z. Zhu, G. Yang, G. An, X. Li, P. Niu, L. Chen, L. Tian, BMP-7 attenuated silica-induced pulmonary fibrosis through modulation of the balance between TGF-β/Smad and BMP-7/Smad signaling pathway, Chem. Biol. Interact. 243 (2016) 72–81, https://doi.org/10.1016/j.cbi.2015.11.012.
[19] D. Merino, A.V. Villar, R. García, M. Tramullas, L. Ruiz, C. Ribas, S. Cabezudo, J. F. Nistal, M.A. Hurlé, BMP-7 attenuates left ventricular remodeling under pressure overload facilitates reverse remodeling and functional recovery, Cardiovasc. Res. 110 (2016) 331–345, https://doi.org/10.1093/cvr/cvw076.
[20] C.A. Narasimhulu, D.K. Singla, The role of bone morphogenetic protein 7 (BMP-7) in inflammation in heart diseases, Cells 9 (2020) 280, https://doi.org/10.3390/cells9020280.
[21] M.M.J. Caron, E.G.J. Ripmeester, G. van den Akker, N.K.A.P. Wijnands, J. Steijns, D.A.M. Surtel, A. Cremers, P.J. Emans, L.W. van Rhijn, T.J.M. Welting, Discovery of bone morphogenetic protein 7-derived peptide sequences that attenuate the human osteoarthritic chondrocyte phonotype, Mol. Ther. Methods Clin. Dev. 21 (2021) 247–261, https://doi.org/10.1016/j.omtm.2021.03.009.

[22] M. Tate, N. Perera, D. Prakoso, A.M. Willis, M. Deo, O. Oseghale, H. Qian, D. G. Donner, H. Kiriazis, M.J. De Blasio, P. Gregorevic, R.H. Ritchie, Bone morphogenetic protein 7 gene delivery improves cardiac structure and function in a murine model of diabetic cardiomyopathy, Front Pharmacol. 12 (2021), 719290, https://doi.org/10.3389/fphar.2021.719290.
[23] E. Martinez-Hackert, A. Sundan, T. Holien, Receptor binding competition: a paradigm for regulating TGF-beta family action, Cytokine Growth Factor Rev. 57 (2021) 39–54, https://doi.org/10.1016/j.cytogfr.2020.09.003.
[24] B. Tampe, D. Tampe, G. Nyamsuren, F. Klöpper, G. Rapp, A. Kauffels, T. Lorf, E. M. Zeisberg, G.A. Müller, R. Kalluri, S. Hakroush, M. Zeisberg, Pharmacological induction of hypoxia-inducible transcription factor ARNT attenuates chronic kidney failure, J. Clin. Investig. 128 (2018) 3053–3070, https://doi.org/10.1172/JCI89632.
[25] A. Schuette, A. Moghaddam, P. Seemann, G.N. Duda, G. Schmidmaier, L. Schomburg, Treatment with recombinant human bone morphogenetic protein 7 leads to a transient induction of neutralizing autoantibodies in a subset of patients, BBA Clin. 6 (2016) 100–107, https://doi.org/10.1016/j.bbacli.2016.08.001.
[26] J. Himmelfarb, G.M. Chertow, P.A. McCullough, T. Mesana, A.D. Shaw, T. M. Sundt, C. Brown, D. Cortville, F. Dagenais, B. de Varennes, M. Fontes, J. Rossert, J.C. Tardif, Perioperative THR-184 and AKI after cardiac surgery, J. Am. Soc. Nephrol. 29 (2018) 670–679, https://doi.org/10.1681/ASN.2017020217.
[27] D. Merino, A. Gil, J. Gómez, L. Ruiz, M. Llano, R. García, M.A. Hurlé, J.F. Nistal, Experimental modelling of cardiac pressure overload hypertrophy: modified technique for precise, reproducible, safe and easy aortic arch banding-debanding in mice, Sci. Rep. 8 (2018) 3167, https://doi.org/10.1038/s41598-018-21548-x.
[28] X.M. Gao, H. Kiriazis, X.L. Moore, X.H. Feng, K. Sheppard, A. Dart, X.J. Du, Regression of pressure overload-induce left ventricular hypertrophy in mice, Am. J. Physiol. Heart Circ. Physiol. 288 (2005) H2702–H2707, https://doi.org/10.1152/ajpheart.00836.2004.
[29] A.C. Midgley, L. Duggal, R. Jenkins, V. Hascall, R. Steadman, A.O. Phillips, S. Meran, Hyaluronan regulates bone morphogenetic protein-7-dependent prevention and reversal of myofibroblast phenotype, J. Biol. Chem. 290 (2015) 11218–11234, https://doi.org/10.1074/jbc.M114.625939.
[30] S. Keller, J. Nickel, J.L. Zhang, W. Sebald, T.D. Mueller, Molecular recognition of BMP-2 and BMP receptor IA, Nat. Struct. Mol. Biol. 11 (2004) 481–488, https://doi.org/10.1038/nsmb756.
[31] M. Mishra, I. Muthuramu, H. Kempen, B. De Geest, Administration of apo A-I (Milano) nanoparticles reverses pathological remodelling, cardiac dysfunction, and heart failure in a murine model of HFpEF associated with hypertension, Sci. Rep. 10 (2020) 8382, https://doi.org/10.1038/s41598-020-65255-y.
[32] J.P. Goetze, B.G. Bruneau, H.R. Ramos, T. Ogawa, M.K. de Bold, A.J. de Bold, Cardiac natriuretic peptides, Nat. Rev. Cardiol. 17 (2020) 698–717, https://doi.org/10.1038/s41569-020-0381-0.
[33] J. Davis, J.D. Molkentin, Myofibroblasts: Trust your heart and let fate decide, J. Mol. Cell Cardiol. 70 (2014) 9–18, https://doi.org/10.1016/j.yjmcc.2013.10.019.
[34] J. Shu, L. Hu, Y. Wu, L. Chen, K. Huang, Z. Wang, M. Liang, Daidzein suppresses TGF-β1-induced cardiac fibroblast activation via the TGF-β1/SMAD2/3 signaling pathway, Eur. J. Pharm. 919 (2022), 174805, https://doi.org/10.1016/j.ejphar.2022.174805.
[35] M. De Vivo, M. Masetti, G. Bottegoni, A. Cavalli, Role of molecular dynamics and related methods in drug discovery, J. Med. Chem. 59 (2016) 4035–4061, https://doi.org/10.1021/acs.jmedchem.5b01684.
[36] D.A. Antunes, J.R. Abella, D. Devaurs, M.M. Rigo, L.E. Kavraki, Structure-based methods for binding mode and binding affinity prediction for peptide-MHC complexes, Curr. Top. Med. Chem. 18 (2019) 2239–2255, https://doi.org/10.2174/1568026619666181224101744.
[37] J. Klages, A. Kotzch, M. Coles, W. Sebald, J. Nickel, T. Müller, H. Kessler, The solution structure of BMPR-IA reveals a local disorder-to-order transition upon BMP-2 binding, Biochemistry 18 (2008) 11930–11939, https://doi.org/10.1021/bi801059j.
[38] X. Chen, J. Xu, B. Jiang, D. Liu, Bone morphogenetic protein-7 antagonizes myocardial fibrosis induced by atrial fibrillation by restraining transforming groth factor-β (TGF-β)/Smads signaling, Med. Sci. Monitor 22 (2016) 3457–3468, https://doi.org/10.12659/msm.897560.
[39] Y. Jin, X. Cheng, J. Lu, X. Li, Exogenous BMP-7 facilatates the recovery of cardiac function after acute myocardial infarction through counteracting TGF-β1 signaling pathway, Tohoku J. Exp. Med. 244 (2018) 1–6, https://doi.org/10.1620/tjem.244.1.
[40] Z. Tong, J. Guo, R.C. Glen, N.W. Morrell, W. Li, A bone morphogenetic protein (BMP)-derived peptide based on the type I receptor-binding site modifies cell-type dependent BMP signalling, Sci. Rep. 9 (2019) 13446, https://doi.org/10.1038/s41598-019-49758-x.
[41] M. Shahid, E. Spagnolli, L. Ernande, R. Thoonen, S.A. Kolodziej, P.A. Leyton, J. Cheng, R.E.T. Tainsh, C. Mayeur, D.K. Rhee, M.X. Wu, M. Scherrer-Crosbie, E. S. Buys, W.M. Zapol, K.D. Bloch, D.B. Bloch, BMP type I receptor ALK2 is required for angiotensin II-induced cardiac hypertrophy, Am. J. Physiol. Heart Circ. Physiol. 15 (2016) 984–994, https://doi.org/10.1152/ajpheart.00879.2015.
[42] M. Dobaczewski, W. Chen, N.G. Frangogiannis, Transforming growth factor (TGF)-β signaling in cadiac remodeling, J. Mol. Cell Cardiol. 51 (2011) 600–606, https://doi.org/10.1016/j.yjmcc.2010.10.033.
[43] N.G. Frangogiannis, Transforming growth factor-β in tissue fibrosis, J. Exp. Med. 217 (2020), e20160103, https://doi.org/10.1084/jem.20190103.
[44] C.Y. Tan, J.X. Wong, P.S. Chan, H. Tan, D. Liao, W. Chen, L.W. Tan, M. Ackers-Johnson, H. Wakimoto, J.G. Seidman, C.E. Seidman, I.G. Lunde, F. Zhu, Q. Hu, J. Bian, J.-W. Wang, R.S. Foo, J. Jiang, Yin Yang 1 suppresses dilated cardiomyopathy and cardiac fibrosis through regulation of BMP7 and CTGF, Circ. Res 125 (2019) 834–846, https://doi.org/10.1161/CIRCRESAHA.119.314794.
[45] H. Khalil, O. Kanisicak, V. Prasad, R.N. Correll, X. Fu, T. Schips, R.J. Vagnozzi, R. Liu, T. Huynh, S.J. Lee, J. Karch, J.D. Molkentin, Fibroblast-specific TGF-β-Smad2/3 signaling underlies cardiac fibrosis, J. Clin. Investig. 127 (2017) 3770–3783, https://doi.org/10.1172/JCI94753.
[46] D. Wnuk, M. Paw, K. Ryczek, G. Bochenek, K. Sładek, Z. Madeja, M. Michalik, Enhanced asthma-related fibroblast to myofibroblast transition is the result of profibrotic TGF-β/Smad2/3 pathway intensification and antifibrotic TGF-β/Smad1/5/(8)9 pathway impairment, Sci. Rep. 10 (2020) 16492, https://doi.org/10.1038/s41598-020-73473-7.
[47] C.K. Nagaraju, E.L. Robinson, M. Abdesselem, S. Trenson, E. Dries, G. Gilbert, S. Janssens, J.V. Cleemput, F. Rega, B. Meyns, H.L. Roderick, R.B. Driesen, K. R. Sipido, Myofibroblast phenotype and reversibility of fibrosis in patients with end-stage heart failure, J. Am. Coll. Cardiol. 73 (2019) 2267–2282, https://doi.org/10.1016/j.jacc.2019.02.049.
[48] G. Marquis-Gravel, B. Redfors, M.B. Leon, P. Généreux, Medical treatment of aortic stenosis, Circulation 134 (2016) 1766–1784, https://doi.org/10.1161/CIRCULATIONAHA.116.023997.
[49] B.A. Aguado, K.B. Schuetze, J.C. Grim, C.J. Walker, A.C. Cox, T.L. Ceccato, A. C. Tan, C.C. Sucharov, L.A. Leinwand, M.R.G. Taylor, T.A. McKinsey, K.S. Anseth, Transcatheter aortic valve replacements alter circulating serum factors to mediate myofibroblast deactivation, Sci. Transl. Med. 11 (2019) 3233, https://doi.org/10.1126/scitranslmed.aav3233.